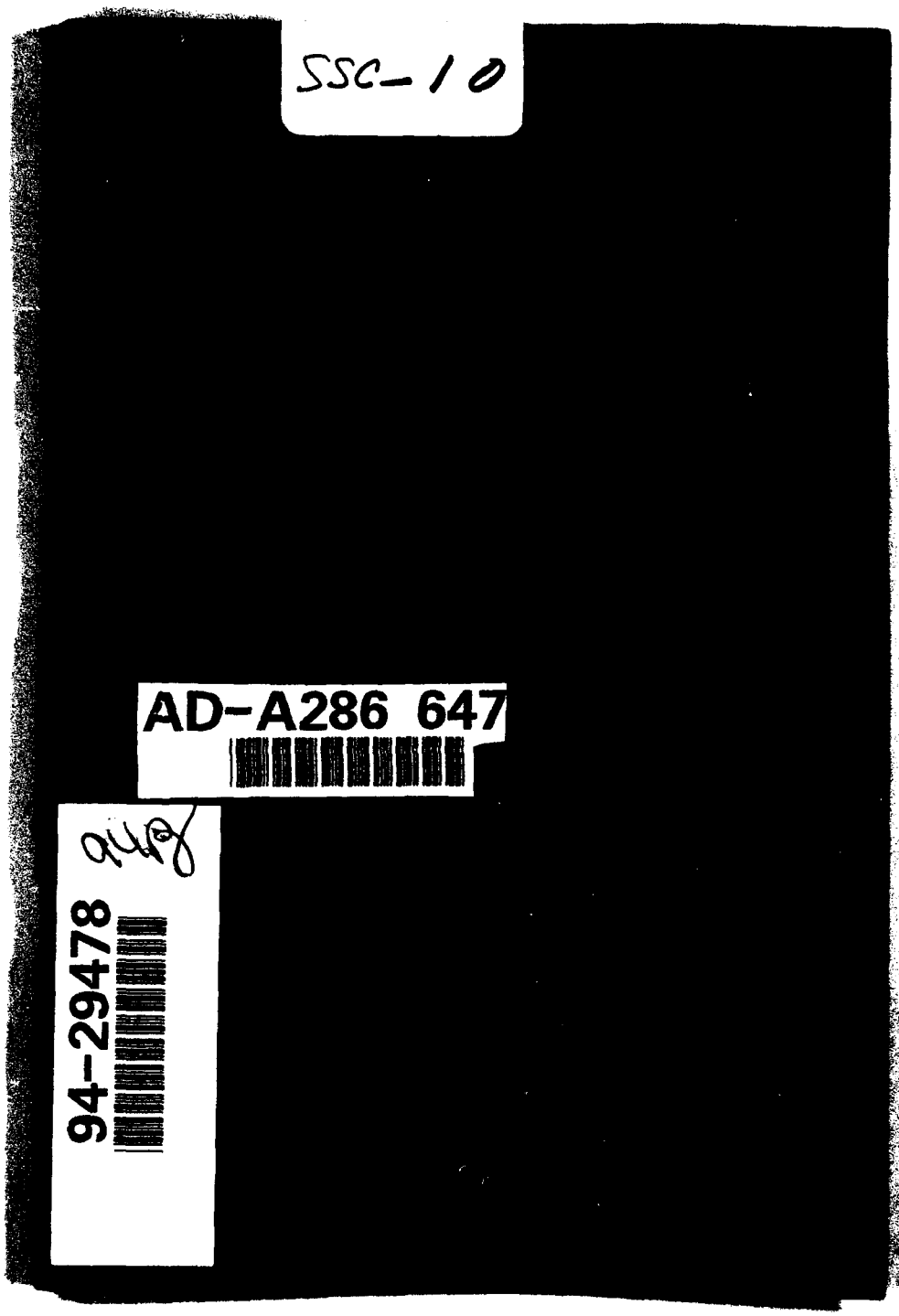
SSC-10
AD-A286 647
94-29478

U.S. Department of Commerce
Frederick H. Mueller, *Secretary*
National Bureau of Standards
A. V. Astin, *Director*

Measurement of Absorbed Dose of Neutrons, and of Mixtures of Neutrons and Gamma Rays

Recommendations of the
National Committee on Radiation Protection
and *Measurements*
NCRP Report No. 25

Accesion For
NTIS CRA&I ☑
DTIC TAB ☐
Unannounced ☐
Justification
By
Distribution /
Availability Codes
Dist | Avail and / or Special
A-1

National Bureau of Standards Handbook 75
Issued February 3, 1961

For sale by the Superintendent of Documents, Washington 25, D.C. - Price 35 cents

Preface

Neutron sources such as nuclear reactors, accelerators, and "radioactive" neutron sources are increasingly a part of modern technology. Neutrons are a special radiation hazard because of (1) their great penetration through matter, and (2) their biological effects. Subcommittee I of the National Committee on Radiation Protection and Measurements has recommended limits for the maximum permissible dose of ionizing radiations (including neutrons) in NBS Handbook 59, as amended on April 15, 1958. Recommendations and rules for protection against neutron radiation up to 30 million electron volts, are given in NBS Handbook 63.

The problems of measurement of neutron radiation are discussed in two handbooks: NBS Handbook 72, "Measurement of Neutron Flux and Spectra for Physical and Biological Applications;" and this Handbook. Methods of measurement of neutron radiation fields involving the physical characteristics of the field such as number flux and energy spectrum are discussed in NBS Handbook 72, while measurements involving energy absorption in matter in neutron and mixed neutron and gamma radiation fields are discussed here. The treatment is rather comprehensive. The information contained here should be helpful in other fields requiring dose measurements such as radiobiology, radiation effects, shielding physics, and reactor physics.

This report was prepared by Task Group No. 1 of Subcommittee M–3 with the following members:

G. S. Hurst, Chairman, Oak Ridge National Laboratory
R. S. Caswell, National Bureau of Standards
F. C. Maienschein, Oak Ridge National Laboratory
H. H. Rossi, Columbia University
J. A. Sayeg, Los Alamos Scientific Laboratory
R. H. Schuler, Mellon Institute
R. W. Wallace, Lawrence Radiation Laboratory

This report has been reviewed for approval by Subcommittee M–3 on "Standards and Measurement of Absorbed Radiation Dose" with the following members:

Members	*Consultants*
H. O. Wyckoff, Chairman	F. H. Attix
G. S. Hurst	M. Berger
H. W. Koch	R. S. Caswell
H. M. Parker	D. V. Cormack
W. C. Roesch	W. Gross
H. H. Rossi	H. E. Johns
G. N. Whyte	F. C. Maienschein
	J. W. Motz
	J. A. Sayeg
	R. H. Schuler
	R. W. Wallace

The following parent organizations and individuals comprise the Main Committee:

H. L. Andrews, USPHS and Subcommittee Chairman.
E. C. Barnes, Amer. Indust. Hygiene Assoc.
C. M. Barnes, Rep. Amer. Vet. Med. Assoc.
J. P. O'Neill, Internl. Assoc. of Govt. Labor Officials.
C. B. Braestrup, Radiol. Soc. of North America and Subcommittee Chairman.
J. C. Bugher, Representative-at-large.
R. H. Chamberlain, Amer. College of Radiology.
W. D. Claus, USAEC.
J. F. Crow, Representative-at-large.
C. L. Dunham, USAEC.
T. P. Eberhard, Amer. Radium Soc. and Subcommittee Chairman.
T. C. Evans, Amer. Roentgen Ray Soc.
G. Failla, Representative-at-large.
J. W. Healy, Health Physics Soc. and Subcommittee Chairman.
P. C. Hodges, Amer. Medical Assoc.
E. R. King, Capt., U.S. Navy.
M. Kleinfeld, Internl. Assoc. Govt. Labor Officials.
H. W. Koch, Subcommittee Chairman.
D. I. Livermore, Lt. Col., U.S. Air Force.
G. V. LeRoy, Subcommittee Chairman.
W. B. Mann, Subcommittee Chairman.
W. A. McAdams, Atomic Indust. Forum and Subcommittee Chairman.
G. M. McDonnel, Lt. Col., U.S. Army.
G. W. Morgan, Subcommittee Chairman.
K. Z. Morgan, Health Physics Soc. and Subcommittee Chairman.
R. J. Nelsen, Amer. Dental Assoc.
R. R. Newell, Amer. Roentgen Ray Soc.
W. D. Norwood, M.D. Indust. Medical Assoc.
H. M. Parker, Subcommittee Chairman.
C. Powell, USPHS.
E. H. Quimby, Amer. Radium Soc. and Subcommittee Chairman.
J. A. Reynolds, Natl. Electrical Mfr. Assoc.
H. H. Rossi, Subcommittee Chairman.
M. D. Schulz, Amer. College of Radiology.
T. L. Shipman, Indust. Medical Assoc.
L. S. Skaggs, Subcommittee Chairman.
J. H. Sterner, Amer. Indust. Hygiene Assoc.
R. S. Stone, Radiol. Soc. of North America.
L. S. Taylor, NBS.
E. D. Trout, Natl. Electrical Mfr. Assoc.
B. F. Trum, Rep. Amer. Vet. Med. Assoc.
Shields Warren, Representative-at-large.
J. L. Weatherwax, Representative-at-large.
E. G. Williams, Representative-at-large.
H. O. Wyckoff, Subcommittee Chairman.

The following are the NCRP Subcommittees and their Chairmen:

Subcommittee	1. Permissible Dose External Sources, H. M. Parker.
Subcommittee	2. Permissible Internal Dose, K. Z. Morgan.
Subcommittee	3. X-rays up to Two Million Volts, T. P. Eberhard.

Subcommittee 4. Heavy Particles (Neutrons, Protons, and Heavier), H. H. Rossi.
Subcommittee 5. Electrons, Gamma Rays and X-rays Above Two Million Volts, H. W. Koch.
Subcommittee 6. Handling of Radioactive Isotopes and Fission Products, J. W. Healy.
Subcommittee 7. Monitoring Methods and Instruments, H. L. Andrews.
Subcommittee 8. Waste Disposal and Decontamination. (This subcommittee has been inactivated.)
Subcommittee 9. Protection Against Radiations from Ra, Co^{60}, and Cs^{137} Encapsulated Sources, C. B. Braestrup.
Subcommittee 10. Regulation of Radiation Exposure Dose, W. A. McAdams.
Subcommittee 11. Incineration of Radioactive Waste, G. W. Morgan.
Subcommittee 12. Electron Protection, L. S. Skaggs.
Subcommittee 13. Safe Handling of Bodies Containing Radioactive Isotopes, E. H. Quimby.
Subcommittee 14. Permissible Exposure Doses under Emergency Conditions, G. V. LeRoy.
Subcommittee M-1. Standards and Measurement of Radioactivity for Radiological Use, W. B. Mann.
Subcommittee M-2. Standards and Measurement of Radiological Exposure Dose, H. O. Wyckoff.
Subcommittee M-3. Standards and Measurement of Absorbed Radiation Dose, H. O. Wyckoff.
Subcommittee M-4. Relative Biological Effectiveness, V. P. Bond.

A. V. Astin, *Director.*

Contents

Measurement of Absorbed Dose of Neutrons, and of Mixtures of Neutrons and Gamma Rays

1. Introduction

This Handbook represents a summary of currently available methods for determining energy absorption in matter as a result of its interaction with neutrons. Since neutrons are almost invariably accompanied by gamma radiation, mixtures of gamma radiation and neutrons are included. Such an endeavor is herein referred to as mixed radiation dosimetry, although the term absorbed dose is reserved to refer to only one of the quantities of interest, namely the specific absorbed energy in a specified medium (e.g., ergs per gram of water). To formalize the definition of dosimetry, it may be stated that any measurement (or calculation) which secures information on the interactions of radiations with matter in such a way that dose can be inferred is an act of dosimetry. On this basis, a detector having an unknown energy response is not a dosimeter, whereas an energy spectrometer may serve as a very useful dosimeter.

Discussions are general wherever possible; i.e., one is in principle just as interested in the application of dosimetry to radiation chemistry and materials damage as in its application to health physics and radiobiology. It is inevitable, however, that most of the detailed examples will be drawn from the latter categories since in these fields it has long been recognized that dosimetry plays an essential role. Prior to the discussions of methods and applications of dosimetry, useful concepts, units, and a brief survey of the fundamentals of the interaction of neutrons and gamma rays with matter will be presented.

The purpose is to discuss only the physical aspects of the interaction of radiation with matter. The reader is referred to National Committee on Radiation Protection Handbook 63 (NBS, 1957) for information on the importance of the Relative Biological Effectiveness (RBE) in protection against neutron radiation. A general discussion of RBE for the protection of persons will be given in section 4.2.

1.1. Concepts and Units of Radiation Dosimetry

Sources of ionizing radiation emit energy in the form of particles (such as neutrons or photons). The number of

particles emitted per unit time, the emission rate, multiplied by the particle energy is equal to the rate of energy emission of the source.

At a given distance from a source there exists a certain flux density (usually called flux) which is equal to the number of particles entering a small sphere per unit time divided by the cross-sectional area of the sphere. The product of this quantity and the particle energy is the intensity (or energy flux density). For a flux density or intensity the energy ultimately delivered to matter of specified composition depends on the type and the energy of the incident radiation. The exposure dose is a measure of the radiation based upon its ability to produce ionization (in air). Its unit is the roentgen, which is defined by the International Commission on Radiological Units (NBS Handb. 62, 1957) as follows:

"1 roentgen is an exposure dose of X- or gamma-radiation such that the associated corpuscular emission per 0.001293 gram of air produces in air ions carrying 1 electrostatic unit of quantity of electricity of either sign."

An X-ray beam for which the exposure dose is 1 roentgen (r) imparts to 1 gram (g) of air approximately 87 ergs. The energy imparted per gram of soft tissue varies from about 94 to 97 ergs for X-ray energies between 100 kv and several Mev. The small magnitude of this variation constitutes one of the advantages of the roentgen unit.

The concept of exposure dose is meaningful not only inside irradiated material but also in a vacuum or in "free air." In the latter circumstance the exposure dose is a useful parameter of the output of X- or gamma-ray sources and it may also be used to characterize radiation fields prior to introduction of a biological object. The concept of exposure dose may not be readily extended to radiations other than electromagnetic radiations and no related quantity for other radiations (particularly neutrons) has been universally accepted. The ICRU has this problem under study but until definite recommendations are available, it will be necessary in the following to employ an informally accepted concept in the most commonly adopted interpretation.

The "first collision dose," $D_f(E)$ per neutron or per photon per square centimeter at energy E is given by

$$D_f(E)=\sum_i\sum_j N_i\,\sigma_{ij}(E)\,\epsilon_{ij}(E) \qquad (1)$$

where N_i is the number of atomic particles of type i that can react with a neutron radiation to produce charged particles.

If the reaction is of type j, the cross section for the process is $\sigma_{tj}(E)$, and the average kinetic energy imparted to the charged particles is $\epsilon_{tj}(E)$.

It should be noted that the above equation yields the total kinetic energy imparted to charged particles and that the expression is meaningful for an arbitrarily small amount of irradiated material. In particular, it is not necessary for the irradiated object to have dimensions that are equal to or even comparable to the range of the charged particles produced.

The experimental determination of the first collision dose, however, is usually done with the detectors operating in the region of charged particle equilibrium (see below). This requires walls of finite thickness with resultant attenuation and scattering of primary radiation. Appropriate corrections (NBS Handb. 62, p. 10, 1957) for these effects are often not made and consequently the reported dose values may differ from the ones given by the above equation. For fast neutrons and gamma rays these differences are usually small (often less than 10%). However, for either thermal neutrons or relativistic neutrons the first collision dose given by eq (2) may differ from the measured one by factors of two or more.

Similar to the exposure dose, the first collision dose exists not only in air but also in irradiated materials. Because of the short range of the charged secondaries from fast neutrons, the first collision dose in irradiated material is practically the same as the absorbed dose (see below).

The physical parameter that is considered to be most closely related to the biological effect is the absorbed dose, which is defined by the International Commission on Radiological Units (NBS Handb. 62, 1957) as:

"The energy imparted to matter by ionizing particles per unit mass of irradiated material at the place of interest."

The absorbed dose depends on geometric and material configuration, and precise experimental determinations must usually be carried out either in a biological object or in a suitable phantom. The instruments employed must not appreciably disturb the radiation field and need therefore to be quite small or tissue equivalent in composition. Many dosimeters do not fulfill these requirements or do so only when substantially modified. In the following descriptions of instruments their adaptability to absorbed dose measurements will be discussed in each case.

559496—61——2

The unit of absorbed dose is the rad and the unit of first collision dose will be taken as the rad.[1] One rad is 100 ergs/g. Because of the general nature of this unit, it may be applied to any ionizing radiation, or to any absorbing medium; the latter should always be specified whenever the rad is employed.

A charged particle traversing matter loses energy at a rate which depends on both the nature of the particle and its energy. The lineal rate of local energy absorption is known as the "linear energy transfer" (LET). A particle of unit charge moving at a velocity corresponding to minimum specific ionization, imparts the minimum LET of approximately 0.19 kev/μ of water. If the charge is greater and the velocity is lower, the LET can reach values of many hundred kev per micron.

1.2. Interaction of Radiation With Matter

To understand how radiation interacts with matter in general or with an instrument designed to measure the radiation, it is desirable to understand first the simplest processes, the action of monoergic radiation on individual atoms.

a. Gamma Radiation

For considerations of dosimetry the three most important interactions of X-or gamma radiation with matter are the photoelectric effect, Compton scattering, and pair production.

(1) *Photoelectric effect.* In the photoelectric effect a gamma-ray photon ejects an atomic electron from one of the electron shells of the atom. The electron receives an energy E_e which is the energy of the photon E_γ less the binding energy B which held the electron in the atom; i.e., $E_e=E_\gamma-B$. The energy B is usually dissipated locally either by fluorescent radiation having low penetration or by the emission of Auger electrons. The photoelectric effect is predominant for low gamma-ray energy and in high atomic number materials. At low energies the cross section (τ) decreases very rapidly as the energy of the gamma ray increases, and it increases rapidly with the atomic number Z of the absorber (about as $Z^{4.5}$). Figures 1 through 4 show the variation of the photoelectric cross section with gamma-

[1] It is felt by some that the unit for first collision dose should be ergs per gram and that the rad should be used only for the absorbed dose. However, others feel that the rad should be used for both quantities. As it is still unsettled, this Handbook will use rads as the unit for both types of dose.

ray energy for the elements hydrogen, carbon, oxygen, and lead. A tabulation of the photoelectric cross section and other gamma-ray interaction cross sections is available (Grodstein, 1957 and Berger, 1960).

(2) *Compton scattering.* The Compton effect predominates over the photon energy range from about 1 to 5 Mev in high atomic number materials and over an even wider range in low atomic number materials. In this process the photon may be thought of as colliding with an electron which is usually considered free (i.e., the binding energy is neglected). The photon is degraded in energy and the scattering is incoherent (no fixed phase relation between the incident and scattered photon). The recoil electron is always ejected in a forward direction. It can be shown that the maximum energy E_{max} of the Compton recoil electron is

$$E_{max}=E_\gamma[1+(m_0c^2/2E_\gamma)]^{-1} \tag{2}$$

$$\cong E_\gamma-\frac{m_0c^2}{2} \text{ (for } E_\gamma \gg m_0c^2) \tag{3}$$

where E_γ is the incident photon energy. Thus for high-photon energy the maximum electron recoil energy is about ¼ Mev less than the incident photon energy. The average fraction of the energy transferred to the electron is the cross section for energy absorption divided by the total Compton cross section and may be conveniently obtained from Davisson and Evans (1952) or from Nelms (1953).

The behavior of the total Compton cross section σ as given by the Klein-Nishina formula is shown in figures 1 through 4. Since in Compton scattering each electron may be considered to be free, the cross section per atom is proportional to atomic number Z.

(3) *Pair production.* A positron-electron pair can be produced when a gamma ray passes through a strong electrostatic field (the field of a nucleus or less frequently that of an atomic electron). Since the energy required to produce the two electron masses is 1.02 Mev, pair production cannot occur below this gamma-ray energy, and for $E_\gamma>1.02$, $E_{pair}=E_\gamma-1.02$, where all energies are in Mev. The cross section for pair production levels off at high energies because of screening of the nucleus by atomic electrons. The pair production cross section varies from element to element approximately as Z^2, and is about 100 barns/atom for the heaviest elements. For specific values of the cross section, see Grodstein (1957) and figures 1 through 4.

The energy absorption coefficients for these processes have been used to calculate the first collision dose for gamma radiation incident upon various media (appendix 1).

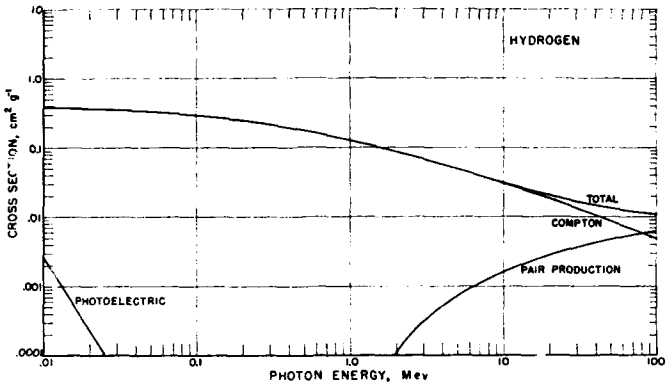

FIGURE 1. *Photoelectric, Compton, pair production, and total cross sections ($cm^2\ g^{-1}$) for hydrogen as a function of photon energy (Mev).*

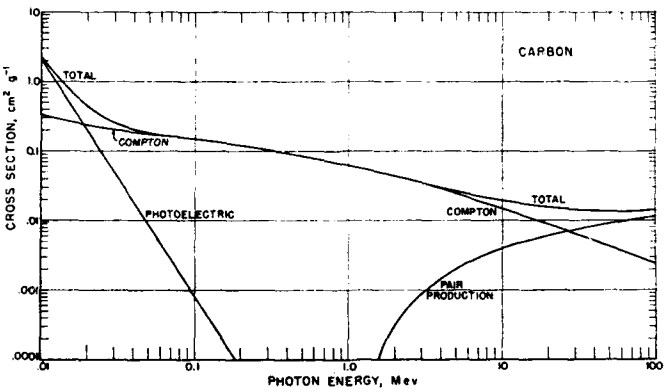

FIGURE 2. *Photoelectric, Compton, pair production, and total cross sections ($cm^2\ g^{-1}$) for carbon as a function of photon energy (Mev).*

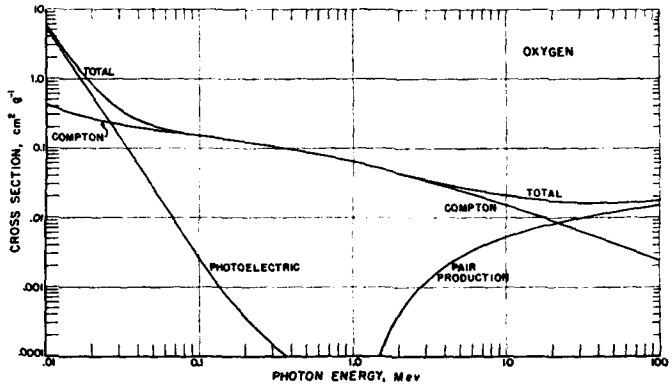

FIGURE 3. *Photoelectric, Compton, pair production, and total cross sections ($cm^2\ g^{-1}$) for oxygen as a function of photon energy (Mev).*

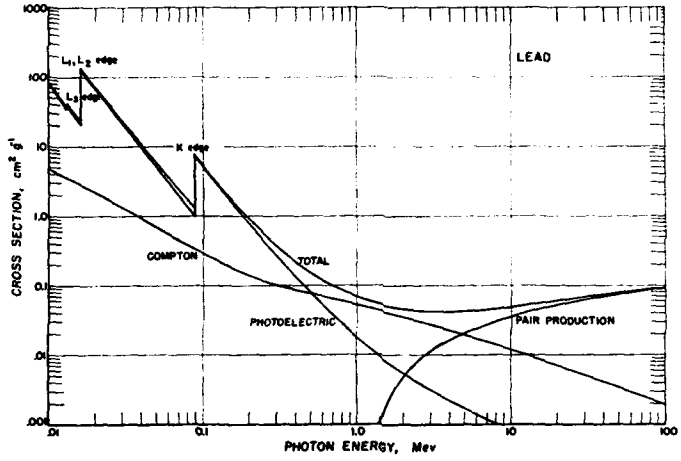

FIGURE 4. *Photoelectric, Compton, pair production, and total cross sections ($cm^2\ g^{-1}$) for lead as a function of photon energy (Mev).*

b. Neutrons

The neutron is a nuclear particle, and may be thought of as interacting with nuclei only. The interaction expected between neutrons and electrons is exceedingly small, and may be neglected for our purposes. The main processes of neutron interactions with the nucleus are:

Elastic scattering: The neutron is scattered and loses energy which appears as kinetic energy of the recoil nucleus. The sum of the kinetic energies of all particles in the system remains constant.

Inelastic scattering: The neutron is absorbed and a neutron re-emitted with loss of energy, leaving the nucleus in an excited state, from which it decays to the ground state by the emission of one or more gamma rays.

Capture: The neutron is captured by the target nucleus, forming a compound nucleus which may be excited and emit gamma radiation.

Reactions producing other particles: The neutron may stay in the nucleus, with other particles such as protons or alpha particles being emitted. At high enough energies, two neutrons may be emitted, or other combinations of particles.

Inelastic scattering, radiative capture, and reactions producing other particles are all examples of *nonelastic reactions* (Goldstein, to be published).

In discussing the interaction of neutrons with matter it is convenient to define four energy groups: Thermal neutrons, intermediate neutrons, fast neutrons, and relativistic neutrons.[2]

(1) *Thermal neutrons.* These neutrons are in thermal equilibrium with matter, and in special cases have a Maxwellian distribution of velocities. In this distribution the most probable velocity per unit velocity at 295° K is 2,200 m/sec, corresponding to an energy of 0.025 ev. The most important interaction with matter is capture. Reactions such as (n,p), (n,α), or fission may occur. In many nuclides the neutron cross section is "$1/v$"; i.e., inversely proportional to the velocity of the neutron. This enables one to measure neutron density (neutrons/cm^3) by the activation of a $1/v$ foil since activation is proportional to $nv\sigma \sim nv\ (1/v) \sim n$. In tissue, the important reactions at low energy are $H^1(n,\gamma)H^2$ which produces a 2.2-Mev gamma ray and $N^{14}\ (n,p)C^{14}$ which yields a 0.6-Mev proton. The $B^{10}(n,\alpha)Li^7$ reaction is very widely used in detectors for low-energy neutrons.

[2] All authors do not use the same limits or names. The present ones are convenient for use in this Handbook.

(2) *Intermediate neutrons (0.5 ev to 10 kev)*. These neutrons are in an energy range where there frequently are large resonance peaks in the neutron cross sections and hence are often called "resonance neutrons". The neutron slowing-down process is an important interaction between intermediate neutrons and matter and leads to a neutron flux inversely proportional to energy (the dE/E spectrum).

(3) *Fast neutrons (10 kev to 10 Mev)*. The most important interaction of these neutrons with matter is elastic scattering. However, in the upper part of this energy range, inelastic scattering and reactions producing other particles account for an appreciable part of the total cross section.

The most important interaction of fast neutrons with tissue is elastic scattering with hydrogen. The neutron and proton have practically the same mass and as a consequence of isotropic scattering in the center-of-mass system, each fraction of the neutron energy is given to the proton with equal probability. In the laboratory system the neutron and proton are emitted at right angles to each other.

The slowing down of neutrons in a moderator is due mostly to the elastic scattering process. The neutron gives at most a fraction $4B/(B+1)^2$ of its energy to the recoil nucleus, where B is the ratio of the mass of the target nucleus to the mass of the neutron. At low-energies elastic scattering is nearly isotropic in the center-of-mass system (at all energies up to 14 Mev in hydrogen), see figure 9. For high B, this implies isotropy in the laboratory as well, since the center-of-mass is moving very slowly. At higher energies elastic scattering is usually not isotropic, often being peaked forward.

Inelastic scattering, which first occurs for most nuclei at an energy of the order of a fraction of 1 Mev, becomes more important as neutron energy increases, and at energies above 10 Mev it may be as probable as elastic scattering. It is important as a source of gamma rays in the neutron moderation process, and causes large neutron energy losses in high B materials where energy losses by elastic scattering can only be small. Examples of total cross sections for hydrogen, nitrogen, carbon, and oxygen are shown in figure 5. A compilation of neutron cross sections is available in U.S. Atomic Energy Commission Report BNL–325. (Hughes and Schwartz, 1958).

Results of calculations of the first collision dose due to fast neutrons incident upon various materials are given in appendix 2.

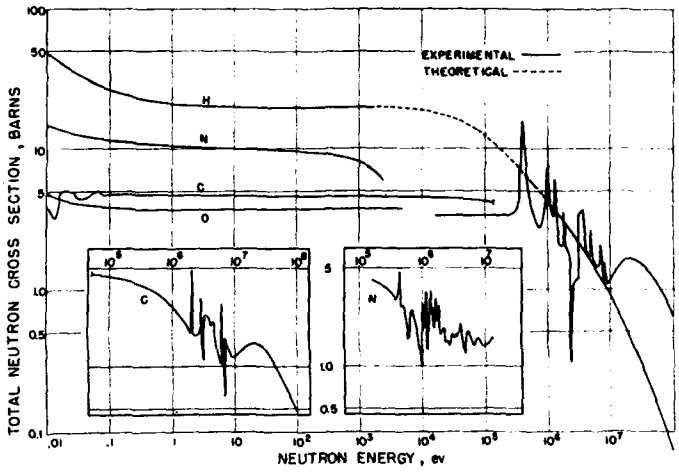

FIGURE 5. *Total neutron cross sections as a function of neutron energy in electron volts for hydrogen, nitrogen, carbon, and oxygen.*

The solid curve indicates a region in which detailed data are available, and the dashed curve represents theoretical interpolation.

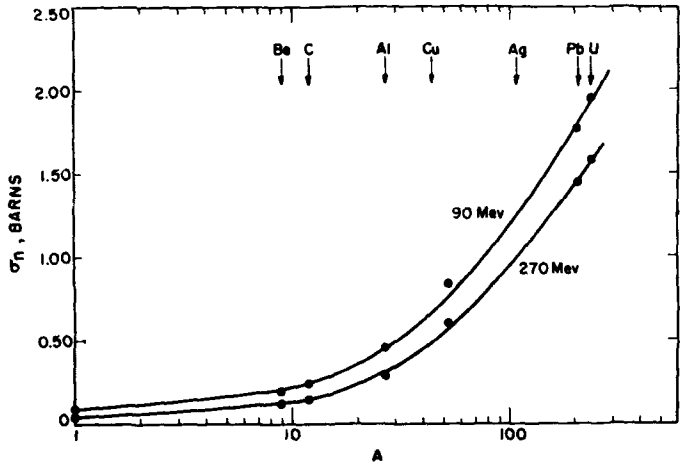

FIGURE 6. *Nonelastic neutron cross sections for elements heavier than hydrogen.*

(De Juren, 1950; De Juren and Knable, 1950; Hess, 1958.)

(4) *Relativistic neutrons.* Neutrons in the relativistic energy range interact differently with matter in several important respects. The discussion which follows is designed to point out these differences. Much of the data necessary for the detailed determination of energy absorption in various materials are not yet available. The information presented in this section should, however, be useful for several reasons; two of these are (1) it provides the reader with a convenient source of experimental data, and (2) it shows that, just as in the case of gamma radiation above 3 Mev, the first collision dose becomes less useful in the case of relativistic neutrons. In order to limit the problem we will only consider the energy range from 10 to several hundred Mev. There are fairly detailed data to about 700 Mev. Meson production does occur in the selected energy range but other unusual events such as strange particle production occur above our top energy limit.

The first important difference between the relativistic region and the fast region is that for neutrons above 20 Mev, inelastic scattering is more important than elastic scattering. Figure 6 gives nonelastic neutron cross sections as a function of the atomic weight A for 90 Mev and 270 Mev (De Juren, 1950; De Juren and Knable, 1950; Hess, 1958). For high A materials the elastic cross section may be neglected since its contribution to the dose is fairly small due to the fact that a small amount of energy is transferred from neutrons to heavy nuclei. For hydrogeneous materials, elastic processes are still important and figure 7 gives the total elastic cross sections for n-p collisions as a function of neutron energy. For comparison, the n-n cross section is also included in this plot (US AEC report AECU-2040, 1952; Hess, 1958; Kruse, Teem, and Ramsey, 1956).

The main form of nonelastic collision is the ejection of protons or neutrons from the target nucleus. At very high energies the energy appearing as gamma radiation is negligible in comparison to the energy of the cascade protons or neutrons. Figure 8 gives the number of protons and neutrons emitted in an elastic event as a function of A for five different energies (Metropolis et al., 1958).[3] The data in figure 8 are based on the assumption that nuclear forces are charge independent.

---

[3] Metropolis et al., (1958) is the best reference presently available from which most of the data contained in this section have been taken. This work is a Monte Carlo calculation which considers cascades within a nucleus and which compares its results with a wide variety of experimental measurements. This comparison indicates that the Monte Carlo technique is quite satisfactory in that the agreement is well within the experimental errors in almost every case. In view of this agreement, it is probable that this fundamental approach of Metropolis et al., is satisfactory for the purpose of calculating doses.

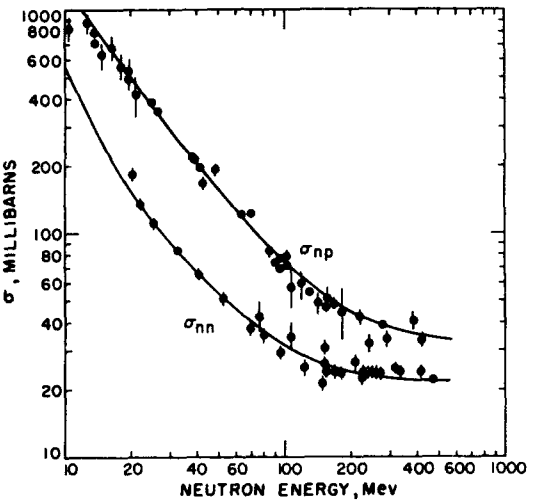

FIGURE 7. *Total elastic n-p and n-n cross sections in millibarns as a function of neutron energy in Mev.*

The solid curves are the analytic expressions used in the calculations (Metropolis et al., 1958), and the experimental points are from US AEC Report AECU-2040 (1952), Hess (1958), and Kruse, Teem, and Ramsey (1956).

The fraction of the dose arising from elastic collisions of relativistic neutrons with nuclei can be roughly estimated by the following considerations. In tissue such collisions would be primarily with carbon, nitrogen, and oxygen. If classical billiard-ball elastic scattering took place, then the recoiling nuclei would have a uniform energy distribution from zero up to $4A/(A+1)^2 \times E_n$, where E_n is the incident neutron energy. Thus, in the case of carbon an incident 1–Mev neutron would produce carbon recoils up to 0.28 Mev and an incident 100–Mev neutron would produce a uniform distribution of recoil nuclei up to 28 Mev. If this situation actually existed for the relativistic neutron the dose from such recoil carbon and oxygen nuclei would have to be taken into consideration. However, this is not the case since the DeBroglie wavelength of neutrons having more than a few Mev is not large compared to the dimensions of a carbon, oxygen, or nitrogen nucleus. Consequently, elastic scattering may not be described by a billiard-ball collision model giving a uniform energy distribution up to the maximum mentioned above, but instead is described by the Fraunhofer

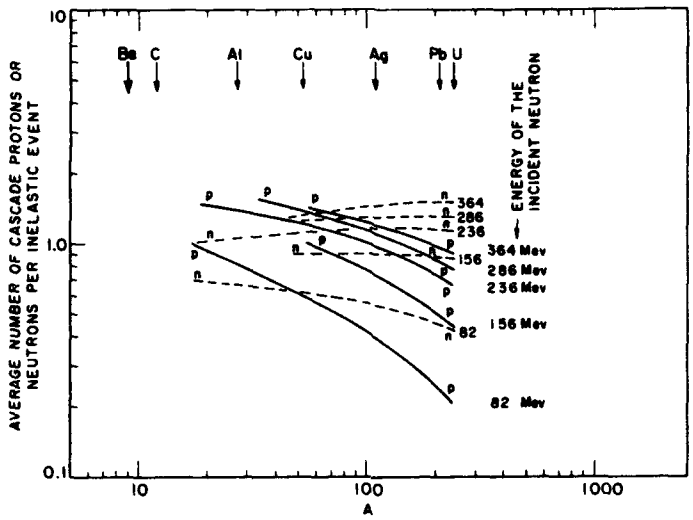

FIGURE 8. *Calculated average number of protons (solid curves) and neutrons (dashed curves) produced per incident neutron for five different bombarding energies as a function of the target nucleus (Metropolis et al., 1958).*

diffraction pattern characteristic of the passage of plane waves over a spherical object whose dimensions are comparable to the wavelength of the incoming wave. For relativistic energy neutrons the Fraunhofer central maximum and even the first side maxima are observed (Moyer, 1954; Amaldi et al., 1946; Bratenahl et al., 1950; Richardson et al., 1952).

The Fraunhofer diffraction pattern differs from the billiard-ball pattern in that the recoiling neutrons are predominantly scattered forward in contrast to the spherical scattering in the center-of-mass system, which is characteristic of the billiard-ball collision. As a result of this forward direction of the neutrons very little energy is imparted to the recoiling carbon, nitrogen, or oxygen nuclei. In fact, a simple calculation shows that the energy distribution of elastically recoiling carbon nuclei which have undergone collisions with 100-Mev neutrons has a simple triangular shape with its maximum at zero energy and extending out to 1 or 2 Mev. The average energy of these carbon nuclei is about 0.3 Mev. It is thus apparent that the wave-mechanical Fraunhofer diffraction type of scattering imparts very little energy to the elastically

recoiling heavy nuclei in most media and as a consequence the dose arising from such elastic processes may be neglected in comparison to the dose arising from nonelastic collisions.

In the case of collisions with hydrogen the data are quite complete and are shown in figures 9 and 10. Figure 9 gives the cross section for *n-p* collisions as a function of the angle in the neutron center-of-mass system for energies from 14.1 Mev to 400 Mev (Hess, 1958). For use in higher order collision calculations, figure 10 is included which gives the *p-p* and *n-n* cross sections as a function of the angle in the center-of-mass system (Hadley and York, 1950). These data for nucleon-nucleon collisions are more complete than the data for higher values of A, even up to the billion electron volt region.

The angular distribution of secondary protons as a function of proton energy at the angles 18°, 25°, and 45° for 90-Mev neutrons incident on copper is given in Metropolis et al. (1958). Such detailed information is not available for other

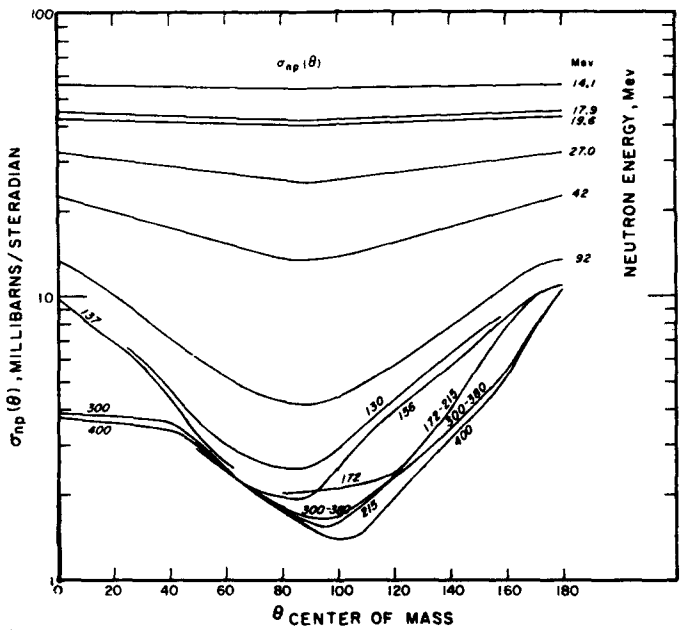

FIGURE 9. *Cross sections for n-p scattering as a function of center-of-mass neutron angle in millibarns per steradian as a function of energy from 14 Mev to 400 Mev (Hess, 1958).*

Errors are about 10 percent

elements with the exception of hydrogen. However, data are available for protons scattered at 40° from aluminum, copper, silver, and bismuth when 96-Mev neutrons are incident (Metropolis et al., 1958). The curves for copper in these two sets of data do not completely agree. This reflects the scarcity of good experimental data on energy and angular distributions of secondary protons.

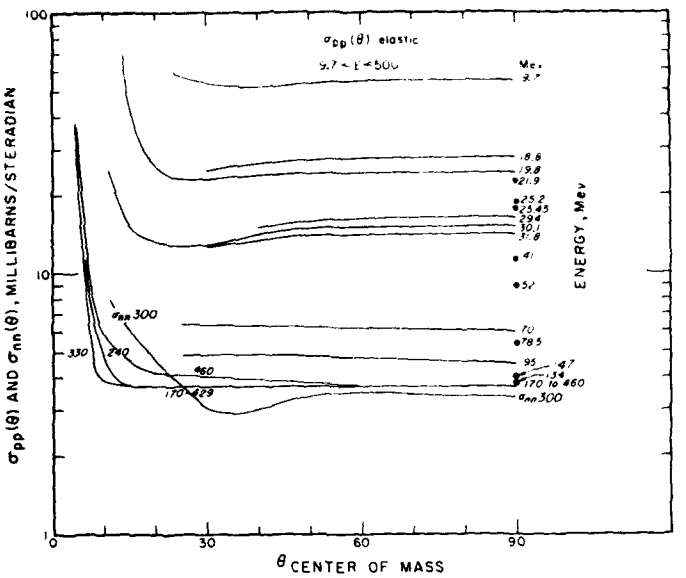

FIGURE 10. *Cross sections for p-p and n-n scattering as a function of center-of-mass angle in millibarns per steradian as a function of energy from 10 Mev to 460 Mev for p-p and at 300 Mev for n-n (Hess, 1958).*

The curves are accurate to about 5 percent.

Figure 11 gives the proton range as a function of energy in various materials (Rich and Madey, 1954). Since the range of several hundred Mev protons is of the order of 10 cm in unit density materials, the first collision dose is not applicable in all applied cases of interest. Thus data for dE/dx are essential to the determination of energy loss to any medium. Figure 12 gives dE/dx for protons as a function of A for energies up to 3 Bev and figure 13 gives dE/dx as a function of residual range in various media.

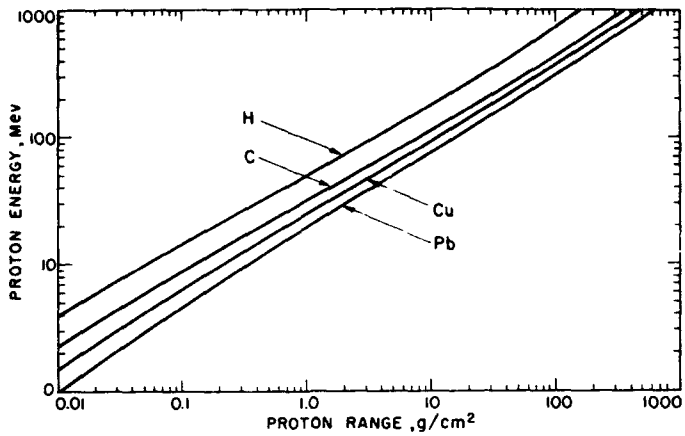

FIGURE 11. *Proton range in g per cm² as a function of energy in various materials (Rich and Madey, 1954).*

2. Methods of Dosimetry

When a beam of neutrons or X-rays strikes matter, secondary charged particles are produced. The density of these secondaries increases up to a depth that equals their maximum range in the material. Beyond this point, charged particle equilibrium is said to exist because the number of secondaries that originates in any layer is approximately equal to the number of those that terminate there. In practice, there is a gradual decrease in intensity of the primary beam due to absorption, while the density of secondaries rises up to the depth where radiation equilibrium is first approached and then falls at the same rate as the intensity of the primary beam is attenuated. If the range of the secondaries is short compared with the attenuation length of the primary radiation, the absorbed dose at the point of radiation equilibrium is approximately equal to the first collision dose. This somewhat simplified picture is usually complicated by the existence of secondaries that accompany the beam before it strikes the material in question, scattering of the primary beam, and the production of tertiary and higher order radiations.

The concept of radiation equilibrium is of considerable importance in ionization measurement of exposure dose and first collision dose. Determinations of these quantities are usually done under conditions of radiation equilibrium, because of difficulties that confront efforts to separate production and absorption of secondary radiation. In such de-

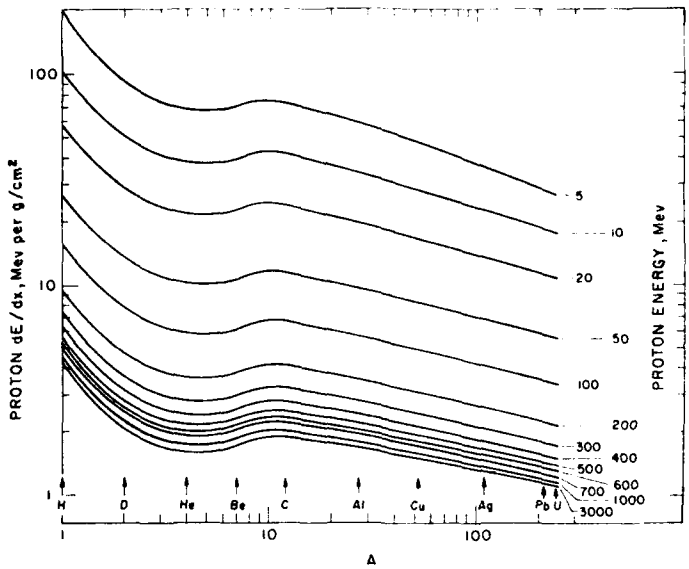

FIGURE 12. *Energy loss for protons in Mev per g per cm² as a function of attenuating material for energies from 5 Mev to 3,000 Mev (Rich and Madey, 1954).*

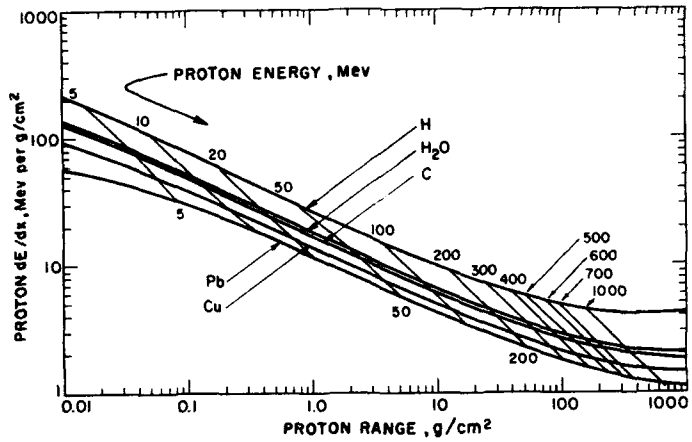

FIGURE 13. *Energy loss for protons in Mev per g per cm² as a function of residual range in various materials with the constant energy lines indicated (Rich and Madey, 1954).*

terminations appropriate corrections are made for absorption of the primary radiation in the transition zone required for establishment of radiation equilibrium.

On the other hand, measurements of absorbed dose may be carried out not only under conditions of radiation equilibrium, but also in the transition zone, since the objective of such measurements is to determine energy locally absorbed rather than energy locally lost from the incident radiation.

2.1. Calorimetry

A very fundamental way to measure absorbed dose is through the temperature rise of the irradiated material. The rise is very small for radiations of interest in biological studies, amounting to only about 2×10^{-6} °C/rad in soft tissue. However, the radiation levels pertinent to studies of radiation damage are sufficiently high so that accurate calorimetric measurements may be readily made. A calorimeter measures the total dose absorbed by the material with no differentiation between neutrons and gamma rays. Some of the energy produced within an irradiated material may be abstracted and used in chemical reactions; conversely, energy could be liberated. Such disturbing effects are expected to be negligible except in special cases. Although, in principle, calorimetry techniques should work equally well for neutrons as for gamma radiation, they have not been applied to the former; hence calorimetry techniques will not be treated extensively in this Handbook. The reader is referred to Milvy et al., (1958) for more information.

2.2. Ionization (Bragg-Gray Principle)

At present, one of the most sensitive methods for determining absorbed dose involves ionization measurements in gases. Since the absorbed dose is defined in terms of energy imparted to a solid, it is necessary to utilize the relation that exists between these two quantities.

If the differential mass of the solid is replaced by gas, the energy imparted to a unit mass of the gas E_g obeys the relation:

$$E_s=S\times E_g, \tag{4}$$

where S is the ratio of the mass stopping power of the solid to that of the gas for the ionizing particles in question. (See NBS Handbook, "Stopping Power for Use With Cavity Chambers", to be published.)

If the average energy required for the production of an ion pair in the gas is equal to W,

$$E_s=SWJ, \tag{5}$$

where J is the ionization per unit mass of gas. This equation, known as the Bragg-Gray relation (Gray, 1936, 1944), is of fundamental importance in measurements of absorbed dose employing ionization methods. It applies only if the following four criteria are met:

(1) The introduction of the gas-filled cavity has a negligible effect on the distribution of charged particles in the medium, which implies that the linear dimensions of the cavity are small compared with the range of these particles in the cavity.

(2) The intensity of primary radiation must be substantially constant in the cavity and in the surrounding wall.

(3) Production of charged tertiary radiations (delta rays) must be the same in wall and gas or the cavity must be large compared with the range of gas-produced tertiaries (Spencer and Attix, 1955).

(4) S and, to some extent, W, are a function of particle type and energy. Mean values for these quantities must be found by proper weighting of the spectrum of charged particles traversing the cavity.

Requirement (1) sets a lower limit to the intensity that may be precisely measured, particularly when the secondaries have a short range. Thus heavy recoils produced by fast neutrons at moderate energy have ranges of the order of 1 mm in air at 0 °C, 760 mm pressure. In an air-filled cavity of reasonable dimensions the pressure must in this case be quite low to conform with requirement (1), resulting in weak currents, even at appreciable intensities.

Requirement (2) is sometimes difficult to fulfill, particularly in the transition layer between the surface and the depth at which the radiation equilibrium is established.[4]

Requirement (3) is usually adequately met when wall and gas are of approximately equal atomic number. If this is not the case, requirement (3) is usually found to oppose requirement (1) to such an extent that reliance must be placed on approximate computed corrections.

Requirement (4) implies a knowledge of the energy distribution of the charged particles in the cavity and its immediate surroundings, a quantity which is usually unknown.

Some of the above requirements are eliminated or much more easily fulfilled if both wall and gas are of the same

[4] The use of Failla extrapolation chamber facilitates measurements in regions of rapidly varying dose.

atomic composition. In this case it will usually be found that S is equal to 1.0 and

$$E_s = WJ', \tag{6}$$

where J' is the ionization per unit mass of wall equivalent gas. In this case requirement (1) is eliminated (Fano, 1954; Rossi and Failla, 1950), requirement (2) remains unchanged, and requirement (3) is automatically fulfilled. Requirement (4) is usually easily met with respect to S. Only if the energy of charged particles is very high (polarization effect) or if it is very low (effects of chemical binding) does S depart significantly from 1.0.

Recent experimental data indicate that W for electrons does not vary markedly with either electron energy or gas. Table 1 shows average values for some gases of interest for dosimetry. These values agree within 2 percent with the data of Jesse and Saudauskis (1955, 1957), Weiss and Bernstein (1955), Bay et al., (1957), Gross, Wingate, and Failla (1956, 1957), and Ovadia et al., (1955), even though the electron energies used by these experimenters varied from an average value of about 5.7 kev up to 17 Mev. No trend with energy is indicated by their results.

TABLE 1. W-*values for electrons, alpha particles, and protons for gases often used in dosimetry*

(Units: electron volts per ion pair)

Particle	Gas				
	Air	O_2	CO_2	CH_4	C_2H_4
Electrons	34.0	31.0	33.0	27.0	26.5
α particles	35.0	32.5	34.0	29.0	28.0
Protons	35.2	(32.8)	34.4		

The alpha particle values in table 1 are for polonium or plutonium sources and the agreement between recent investigators (Jesse and Saudauskis, 1955; Scharpe, 1952; Haeberli et al., 1953; Schmieder, 1939; and Bortner and Hurst, 1953, 1954) is well within 2 percent. However, for lower alpha energies, the values are larger (Jesse and Saudauskis, 1955). When W is determined in air from small energy losses near 5 Mev, the value is approximately equal to that for electrons (Bay and Newman, to be published).

Table 1 also lists some data for 2-Mev protons (Larson, 1958). The value for oxygen was obtained from data relative

to argon (Bakker and Segre, 1951) by using the argon value of Larson.

It is seen from the table that there is only a small difference in W for alpha particles, protons, and electrons; although from gas to gas the change for a given particle is much larger. The difference in the value of W for the indicated particles and between the gases is real; but for a given gas in which all three particles may be present, one might use an average value for the calculation of the absorbed dose in the gas. If the relative percentages of each particle are known and if extreme precision is required, a small correction can be made for variation of W with particles.

The W value for a mixture of two gases is difficult to predict, even when the W value for the pure gases is known. Various equations relating the W for a mixture to the W for pure gases have been used and are summarized by Valentine and Curran (1958). Essentially, one must know an empirical constant for each mixture of gases. The magnitude of this constant has been determined for a number of gas mixtures of interest to dosimetry (Bortner and Hurst, 1954; Moe, Bortner, and Hurst, 1957).

2.3. Chemical Systems

a. Photographic

Photographic film may be used for quantitative dosimetry only if calibrated in terms of a primary or secondary standard. Many elements may be present, including C, H, Ag, Br, and others. In general, film is much more sensitive to gamma rays than to neutrons on the basis of absorbed dose in tissue. Film blackening (density) is widely used for gamma-ray dosimetry, often in the presence of neutrons.

The energy transferred by ionizing radiation to the photographic emulsion initiates the reduction of the silver halide crystals (grains) of the emulsion to atomic silver. The microscopic silver specks formed in this way are referred to as latent image. Upon processing in special developing solutions, these silver specks then serve as nuclei for a massive reduction process, leading to the formation of massive silver aggregates which increase the opacity of the developed photographic emulsion.

The increase in emulsion opacity (or in optical density, which is equal to the logarithm to the base 10 of opacity) is usually measured by photoelectric means. By appropriate calibration procedures, optical density can be related to absorbed dose.

Charged particles transfer their energy to the silver halide grains mainly through collisions leading to atomic excitation and to ionization along the paths of the particles. The photographic effect of charged particles increases with the range of the particles in the emulsion, and—for a given range—with their specific ionization, until one single interaction with a silver halide grain is sufficient to make this grain developable. Any further increase in specific ionization leads to a decrease in the number of grains made developable for any given amount of energy dissipated within the emulsion. Photons, neutrons, and other uncharged particles lose their energy to the emulsion largely through the ionization produced by their charged secondaries.

Whether or not developed photographic density [5] is proportional to absorbed electron energy in the original AgBr is an unsettled question (Hoerlin, 1949; Bromley and Herz, 1950; Greening, 1951). However, for X-ray energies of more than 300 kev, photographic film may be used directly to obtain the absorbed dose in tissue. Below this energy the ratio of the energy absorption in film as evidenced by photographic density to that absorbed in tissue may be as large as 10, due to the presence of high atomic number elements in the emulsions.

Thermal neutron dosimetry based on film blackening may be accomplished by use of appropriate loadings or radiators of elements with large thermal neutron cross sections. Methods of fast neutron dosimetry based on blackening are seldom used. However, since about 85 percent or more of the fast neutron absorbed dose in film results from proton recoils, one can obtain a good measure of the absorbed dose by counting and measuring the range of proton tracks in the emulsion (Dudley, 1956). The absorbed dose is equal to the number of recoil protons times the energy of each. This analytical procedure is tedious and may be greatly simplified by adding appropriate materials adjacent to the film so that counting the number of tracks alone is sufficient to obtain the absorbed dose (Cheka, 1954).

b. Liquid Chemical

Some chemical systems are sensitive enough to detect absorbed doses as low as a few rads. Unfortunately for the most sensitive chemical systems, the relationship between absorbed dose and observable effect is nonlinear.

---

[5] Photographic density is a measure of the "blackness" (incident on the film), and is defined as the logarithm to the base 10 of the ratio of the radiant flux incident to the film to the flux transmitted by the film.

Radiation chemical yields are usually expressed on the molecular scale, e.g., in terms of values for G (the symbol usually used for radiation yield) which is the number of molecules produced per 100 ev of absorbed energy; thus,

$$\text{Absorbed energy in ev} = \frac{\text{Chemical reaction (i.e., molecules produced)}}{G} \times 100. \quad (8)$$

The chemical change corresponding to the absorption of 1 rad can be calculated from the above definition of G. Thus,

$$\text{Dose in rads} = \frac{\text{Reaction product concentration in moles/liter}}{1.04 \times d \times G \times 10^{-9}}, \quad (9)$$

where d is the density of the chemical system in g/cm^3. If the radiation yield is constant during the reaction then the observed chemical change will be proportional to the absorbed dose and the absolute sensitivity of the dosimeter can be given in terms of this value. In many chemical systems, however, changes in the chemical composition resulting from radiolysis lead to a change in yield and therefore to a non-linear response of the dosimeter.

It is necessary that the radiation yield be independent of LET over the range of interest, and this introduces some difficulties for radiations characterized by a high LET. Measurements on aqueous systems for particles having an initial LET greater than 5 kev/μ have shown that the fundamental radiation chemical processes are considerably different from those produced by radiations of lower LET. At low LET the predominant primary products are hydrogen and hydroxyl radicals and at high LET, molecular hydrogen and hydrogen peroxide. In general, it may be expected that in aqueous systems the observed yields will necessarily be dependent on the nature of the radiation and therefore any possible use of these systems in the dosimetry of mixed radiations requires a broad knowledge of the radiation chemical yields as a function of LET together with detailed information on the energy spectrum of the radiations actually present in the dosimeter. For radiations having a LET less than 1 kev/μ, the radiation yields for aqueous systems are effectively independent of LET. Preliminary investigations on the radiochemistry of aliphatic hydrocarbons with particles having a LET as high as 50 kev/μ have not indicated a dependence of yield on LET. These systems there-

fore show promise for the total energy dosimetry of radiations of high LET although at the present time they are not sufficiently sensitive in the region of interest in radiobiological investigations.

Since for reactions which do not involve chain mechanisms the values of G are usually less than 10, the observable chemical changes are less than 10^{-8} moles/liter/rad. Because such small amounts of reaction products are very difficult to detect, chemical dosimetry involving these systems is usually restricted to work at high radiation levels.

A number of attempts have been made to utilize chain reactions. The chemical chain reaction is one in which the product of the reaction will induce further chemical reactions. Therefore, it is characterized by a high chemical yield per unit of absorbed energy. These systems are, however, very sensitive to impurities and usually have yields which are dependent upon LET and intensity.

2.4. Spectral Measurements

For both fast neutrons and gamma radiation it is possible to calculate the energy absorbed per gram of the irradiated medium as a function of radiation energy. This calculation is particularly simple for cases where radiation equilibrium (see sec. 2) has been established. It is sometimes practical to carry out radiation dosimetry by measuring the spectrum of the radiation, $n(E)$, and then calculating the first collision dose, D_f, by means of

$$D_f = \int_0^\infty n(E)\, D_f(E) dE, \tag{10}$$

where $D_f(E)$ is defined in section 1.1. Obviously, $n(E)$ must refer to the actual energy spectrum at the point in the medium where D is to be determined. Curves and tables for $D_f(E)$ are given in appendix 1 for gamma radiation in various media, and examples of $D_f(E)$ for fast neutrons are shown in appendix 2. Methods of measuring $n(E)$ for fast neutrons are treated in detail in NBS Handbook 72.

2.5. Special Counting[6] Methods

Each of the above experimental methods of dosimetry utilize principles based on rather fundamental relationships

[6] Counting devices in which the pulses must be weighted in proportion to their height to obtain the energy absorbed in the gas-filled cavities are based on the Bragg-Gray principle and do not fall in the present category.

between energy absorbed in the detecting medium and some observable effect in the medium. Thus calorimetry involves a relationship of temperature to energy absorbed, the Bragg-Gray principle owes its success to the empirical fact that W is nearly independent of particle energy, and chemical methods utilize known relationships between the amount of some chemical product and the energy absorbed in the system. These fundamental relationships are then used to determine the energy absorbed in the irradiated system. Only in special cases can the energy absorbed in some other medium be determined from these measurements of the energy absorbed in the irradiated medium.

Direct indication of the dose received by a specified medium may be obtained simply from the number of counts in a detector, i.e., the ratio of the energy absorbed per gram of a medium of interest to the number of counts is independent of the energy of the radiation. In using this method the materials making up the detector may bear little or no resemblance to the medium for which the energy absorption is indicated. For example, the tissue dose may be indicated by simply determining the number of counts in specially constructed proportional counters, even though the materials making up the counter are not in any sense tissue equivalent, and even though the count rate is not proportional to the rate of energy absorption in the counter. Section 3.4 describes a number of instruments based on the counting method. The method is usually applied in those cases where the dose per unit flux versus energy relationship for the medium of interest is known.

3. Instruments and Methods for Determination of Dose

3.1. Ionization Devices

Absorbed dose may be accurately and conveniently determined with ionization cavities employing the Bragg-Gray relation.

a. Ionization Chambers for Measurement of Neutrons and Gamma Rays

The tissue equivalent ionization chamber (Failla and Rossi, 1950) may be used to determine the total absorbed dose in tissue, and other instruments must be used to evaluate the relative proportions of the radiations making up this total dose. Its sensitivity to neutrons is within 10 percent or less of its sensitivity to gamma rays, the difference being due to the difference in W for the two cases.

The degree to which the atomic composition in tissue needs to be duplicated depends not only on the desired accuracy of the measurement but also on the type of radiation that is to be measured. For most of the spectrum of electromagnetic radiation, plastics represent a reasonably good substitute, while in the case of neutrons the hydrogen content of the plastic employed is very critical (Shonka et al., 1958). Plastics are available which contain either 7 percent or 14 percent hydrogen by weight. If the latter type, specifically polyethylene, is mixed with graphite, the hydrogen content is lowered and at the same time the material is rendered electrically conductive, which obviates the need of conductive coatings on the interior of the chamber. In addition, it is possible to add nitrogen-containing compounds to the mixture. This is of importance if the chamber is to respond properly to intermediate or thermal neutrons. A plastic (Rossi and Failla, 1956) has been developed with the following composition:

Hydrogen	10.1 percent
Nitrogen	3.5 percent
Carbon and traces of oxygen	86.4 percent

(percentages by weight)

This material differs in atomic composition from tissue only in that oxygen is almost entirely replaced by an equal weight of carbon. Experiments have indicated that for fast neutrons in the range from about 0.5 to 14 Mev such a substitution results in an error of no more than 6 percent (Rossi and Failla, 1956). A tissue equivalent gas mixture that can be used in a chamber having this wall material is:

Methane	64.4 percent
Carbon dioxide	32.4 percent
Nitrogen	3.2 percent

(percentages per partial pressure)

If exact tissue equivalence is required, it is possible to construct chambers lined with tissue equivalent gels matching a tissue composition $(C_6H_{40}O_{18}N)_a$ exactly. The mixtures employed for one of these as well as other tissue equivalent materials (gaseous and liquid) are given by Rossi and Failla (1956).

Tissue equivalent ionization chambers have been built that operate satisfactorily from dose rates of less than 1 mr/hr to dose rates as high as several thousand rads per minute. Figures 14 and 15 show cross sections of high- and low-sensitivity chambers, respectively.

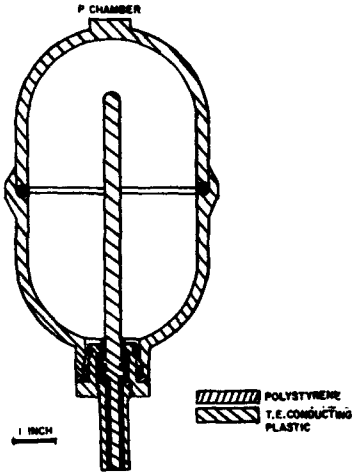

FIGURE 14. *Schematic of a large size (high sensitivity) tissue equivalent ionization chamber.*

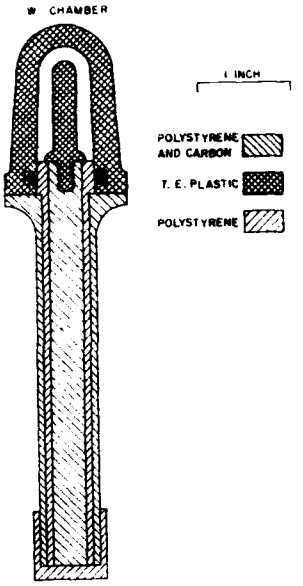

FIGURE 15. *Schematic of a small size (low sensitivity) tissue equivalent ionization chamber.*

Approximate methods have been devised that permit evaluation of a radiation field in terms of its component primary radiations, especially with regard to the separation of doses due to neutrons and gamma rays. Ionization chambers lined with carbon or conducting teflon and filled with carbon dioxide (Rossi and Failla, 1956) may be expected to yield a good measure of the absorbed dose delivered to tissue by electromagnetic radiations, while being rather insensitive to neutrons. However, these devices have a certain neutron sensitivity, k. The coefficient k may be defined as the ratio of the reading of a teflon-CO_2 chamber exposed to a neutron flux which delivers 1 rad to standard tissue, to the reading observed when the chamber is exposed to 1 r of hard X-rays. Experimental and computed values of k are given in table 2. The former were obtained with a chamber made of conducting teflon and filled with carbon dioxide gas having the cross section shown in figure 15,

utilizing neutron beams having minimal gamma contamination. However, since the presence of gamma radiation can not be excluded, these figures must be considered as upper limits only. The computed values for k were obtained by calculations of the type given in appendix 2 and with the assumption that W is the same for heavy recoils as for protons. They are, therefore, also upper limits, although for a different reason.

When a tissue equivalent ionization chamber is exposed to 1 r of reasonably hard electromagnetic radiation, the absorbed dose is approximately 0.97 rads. Because of a difference in W an equal amount of charge will be collected when the chamber is exposed to a neutron dose of 1.03 rads. When a teflon-CO_2 chamber is exposed to 1 r of X-rays of the same energy the corresponding absorbed dose for tissue remains 0.97 rads. However, when this chamber is exposed to 1 rad of neutrons the relative reading will be k.

TABLE 2. *Maximum* k (*r/rad*) *for a teflon-CO_2 chamber* [a]

Neutron energy	Observed k	Computed k
Mev	r/rad	r/rad
0.5	0.08	0.11
1.0	.08	.18
2.0	.09	.13
3.0	.12	.10
4.0	.15	.15
6.0	.20	.16
8.0	.24	.20

[a] See text for limits of accuracy.

If both chambers are exposed in a mixed radiation field and T and C represent, respectively, the tissue equivalent and teflon chamber deflections, relative to the ones caused by 1 r of X-rays, it will be seen that:

$$T=0.97N+1.03\Gamma \tag{11}$$

$$C=kN+1.03\Gamma \tag{12}$$

where N and Γ are the neutron and gamma tissue doses in rads. This procedure makes it possible to evaluate the mixed radiation field on the basis of X-ray calibrations of the two chambers. Direct calibrations may be performed on an absolute basis taking into account chamber volume, gas pressure, electrical capacity, W, and the voltage sensitivity of the detector.

Use of the paired chamber technique requires a reasonably accurate knowledge of neutron energy, if precision is required. If the neutron energy is unknown, k may be assumed to be equal to 0.16. It can be shown that in the range from 0.5 to 8 Mev this choice can introduce a maximum error of approximately 10 percent in the neutron dose regardless of the ratio of neutron dose to gamma dose. On the other hand, the error in the gamma dose depends on this ratio and ranges from negligible values when the gamma dose is very high to errors of the order of 100 percent when the gamma dose becomes less than 10 percent. However, in addition to uncertainties in k, additional errors are introduced in the assessment of the neutron dose when the gamma dose is high, because in this case the neutron dose is evaluated as a result of the subtraction of two numbers which are very nearly equal.

The ratio k decreases with decreasing neutron energy and becomes negligible below 100 kev. In measurements involving low energy fast neutrons, intermediate neutrons or thermal neutrons, a multiple ionization chamber technique permits a rather precise measurement. In particular, in the case of thermal neutrons the teflon-CO_2 chamber will only register contaminant gamma radiation. Tissue equivalent ionization chambers devoid of nitrogen (*TE–N* chambers) (Rossi and Failla, 1956; Rossi, 1956) will register contaminant gamma radiation, as well as gamma radiation arising from capture of hydrogen in tissue, while the tissue equivalent chamber will also register protons from neutron capture in nitrogen. Thermal neutrons produce intense and penetrating gamma radiation in tissue and for this reason the absorbed dose in tissue masses of dimensions in excess of 1 cm is larger than the first collision dose of neutrons and depends on the size of the irradiated object. Absorbed dose measurements must be performed in phantoms using chambers made of tissue equivalent plastic. *TE–N* and teflon liners should have only sufficient thickness to absorb all protons.

A number of similar schemes (Gray, Mottram, and Read, 1940; Dainty, 1950; Bretscher and French, 1944; Marinelli, 1953) involving several ionization chambers have been devised in attempts to separate neutron and gamma doses.

b. Proportional Counters for Measurement of Absorbed Dose Due to Fast Neutrons

Proportional counters may be used to advantage in measuring fast neutron dose in the presence of gamma rays (Hurst, 1954). The Bragg-Gray cavity principle is applied; for example, ethylene gas and polyethylene liners are satisfactory for fast neutrons since the ratio of energy deposited per gram of ethylene to energy dissipated per gram of tissue

is substantially independent of neutron energy. The essential departure from the ionization chamber technique is that the number of ion pairs produced in the gas is determined by a summation of pulse heights, rather than an integration of charge or a current measurement. This fact enables one to integrate only the pulses due to neutrons while rejecting those due to gamma rays, if the dimensions of the gas cavity and the pressure of the gas are chosen so that the pulses due to electrons (from gamma-ray effects) are generally smaller than most of the pulses due to recoil protons (from fast neutron collisions). If the pulse height is proportional to the number of ion pairs formed, this method of dosimetry is in every way equivalent to the ionization chamber, with the added advantage of being quite insensitive to gamma radiation.

The proportionality between pulse height and number of ion pairs depends on two conditions: (a) There must be no electron attachment, and (b) the height of the pulse at the output of the linear amplifier must not depend on track orientation. Condition (a) may be fulfilled by excluding from the counter such gases as water vapor, oxygen, and some of the halogens, which have very large electron attachment cross sections (Healey and Reed, 1941). Condition (b) may be fulfilled by proper selection of the amplifier rise time and decay time (Hurst and Ritchie, 1953). A variation of the angle between the recoil proton trajectories and the center wire in a proportional counter causes a variation in the pulse profiles. However, it has been shown (Hurst and Ritchie, 1953) that if the rise time and decay time constants (assumed to be equal, which is true for many good linear amplifiers) (Jordan and Bell, 1947) are greater than the collection time of electrons in the counter, the pulse height at the output of the amplifier depends only slightly on the rise time of the proportional counter pulse.

Several variations of proportional counters following these principles have been designed. One of these (fig. 16) contains an internal alpha source for calibration. Since the sensitive volume is determined by means of field tubes (Cockroft and Curran, 1951), the mass of gas is known and hence the sensitivity of the detector can be determined without using a known neutron source. The count rate versus pulse height curve produced by Po-Be neutrons impinging on the "absolute" counter is shown in figure 17. Since dose is proportional to the summation of pulse heights, it is also proportional to the area under the count rate versus integral pulse height curve. The area may be accurately

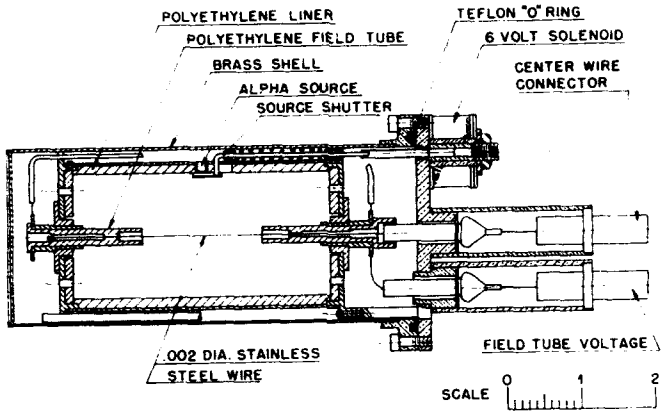

FIGURE 16. *Drawing for the absolute fast neutron dosimeter.*
The proportional counter is lined with polyethylene and filled with ethylene. Field tubes define the active volume, and use of an α source permits direct determination of Mev/g of ethylene.

determined with a planimeter or the summation of pulse heights may be done directly with an electronic pulse integrator (Glass and Hurst, 1952). Direct calibration may be made by means of the curve shown for alpha particles.

The data illustrated in figure 17 correspond to the case where the ratio of the tissue dose due to Co^{60} is approximately 40 times the tissue dose due to Po-Be fast neutrons. If the neutron energy lost under the bias, B (B=5 v in this case) were not taken into account, the area, A_1 would represent the energy lost, and the fraction of energy lost, f, would be $A_1/(A_1+A_2)$. In the case considered this fraction is 0.040; hence the error which would be made by neglecting the energy lost under the bias would be 4.0 percent. Values for f for various values of the bias, B, and neutron energies, E, are given in table 3.

TABLE 3. *Percent, f, of energy spent by recoils losing less than the bias energy, B, in the counter*

Bias		Fast neutron energies							
Energy	PHS-volts (fig. 17)	0.5 Mev	1.0 Mev	2.0 Mev	3.5 Mev	4.8 Mev	14 Mev	Po-B	Po-Be
Mev									
0.074	2.6	8.9	2.0	1.5	1.3	1.4	2.5	0.6	1.4
.14	5.3	19.5	9.4	4.1	3.5	2.8	8.5	2.8	4.5
.21	7.8	32.0	12.9	7.6	5.6	5.9	16.2	6.5	10.1
.28	10.5	52.6	23.5	12.3	9.1	9.8	25.8	9.9	14.4
.36	13.2	73.0	33.3	18.8	12.8	16.2	36.9	15.2	20.5

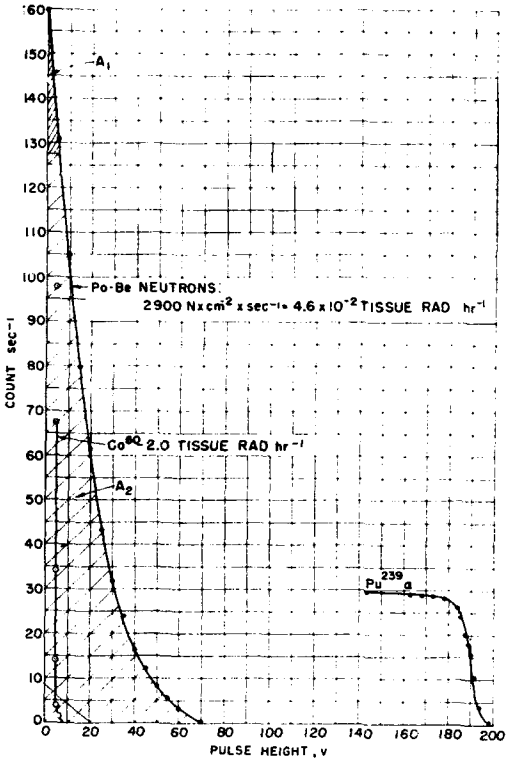

FIGURE 17. *Integral count rate as a function of pulse height for Po-Be neutrons incident upon the absolute counter.*

When using the absolute proportional counter with conventional electronic equipment, the value of B may be chosen to suit the particular experimental conditions (Wagner and Hurst, 1959). Factors which govern the choice of B include the following: neutron energy, neutron intensity, gamma-ray energy, and gamma-ray intensity. In any case the discrimination level at which the results may be appreciably affected by gamma radiation may be determined directly for the particular experimental conditions. Figure 18 shows how this is accomplished in atypical case (1 mrad/hr fast neutron dose rate (Po-Be) and various values of Co^{60} gamma-ray dose rate, ranging from 1 r/hr to 100 r/hr).

For example, for gamma-ray dose rates of 1 r/hr or less the bias level required to discriminate against gamma rays is about 0.20 Mev, and the percent of absorbed neutron energy which would be lost under this bias is about 10 percent (see table 3). On the other hand, if the gamma dose rate were as high as 25 r/hr, the bias level would have to be increased to about 0.36 Mev and the energy lost would be about 20 percent. It should be noted that this energy lost may be estimated by simply plotting the data in the form illustrated in figure 18, extrapolating the count rate

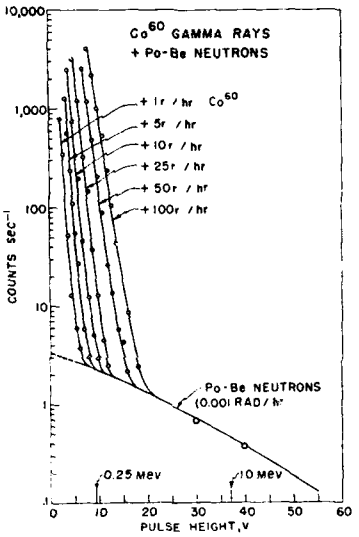

FIGURE 18. *Counts per second versus integral pulse height for mixtures of Co^{60} gamma rays with Po-Be neutrons.*

versus pulse height curve for values of pulse height $\leq B$ and then integrating the area under the entire curve. In other words, the values for f given in table 3 do not necessarily represent errors in the measured dose, but do represent the fraction of the total dose which must be estimated by extrapolation.

In order to indicate the limitations of the proportional counter method in separating neutrons from large dose rates of gamma radiation, results for a very severe case (0.5-Mev neutrons with X-rays of 200 kev effective energy) will be quoted. Again, if the neutron dose rate is taken to be 1

mrad/hr, the bias level must be greater than 0.20 Mev for 1 r/hr 200 kev (effective) X-rays, but f is now 32 percent. For an X-ray dose rate equal to 5 r/hr, the required bias is 0.28 Mev and f is 53 percent. Even this case would not be likely to lead to difficulty in practice since X-rays in this energy range could easily be attenuated by shielding with high Z materials.

A particularly convenient instrument (Wagner and Hurst, 1958) utilizing the absolute counter has been developed. In this instrument, the pulse integrator is a simple four-stage binary circuit (Glass and Hurst, 1952) which gives the area under the integral pulse height curves with very good accuracy, considering the extreme simplicity of the circuit. The ratio,

$$H=\frac{\text{Indicated pulse height summation}}{\text{True pulse height summation}}, \qquad (13)$$

is 1.00 ± 0.08 over a range of neutron energies from 0.5 to 14.0 Mev. In this case energy losses under the bias are partially compensated in the integration process. Output signals from the pulse height integrator are fed into an indicating system which uses decade scalers, preset timers, and lamps serving as decimal indicators in such a way that the dose rate is indicated in mrad/hr. When using this scheme of pulse height integration, the gamma response considerations mentioned above do not hold. Experimental results for the case of Co^{60} have been reported by Wagner and Hurst (1958).

Another proportional counter (Hurst, 1954) is a simple design which is calibrated either with a known neutron source, using collision calculations, or by comparison with the absolute counter. The latter instrument was designed primarily for making measurements in tissue equivalent phantoms and for similar applications. A design which is useful for high intensity neutron measurements, such as produced by cyclotron radiation, has been described by Hurst et al., (1956b). This counter, when used with electronic equipment having a resolving time of 5 μsec, is capable of measuring up to about 10 rads/min with less than 5 percent counting loss, whereas the corresponding dose rates for the absolute counter and the phantom counter are about 0.1 rad/min and 1 rad/min, respectively.

Proportional counters similar to the above have been used to measure the fast neutron dose as well as the total (neutron + gamma) dose in mixed beams (Slater, Bunyard, and Randolph, 1958).

c. Proportional Counter for Measurement of Gamma Radiation Only

A proportional counter may be used as a dosimeter for gamma rays in the presence of neutrons by pulse height integration of the small pulses due to gamma rays and rejection of the large pulses due to neutrons (Caswell, 1960). This approach is opposite to that of the proportional counter for fast neutron dosimetry. This instrument consists of a graphite wall, helium-CO_2-filled proportional counter operated at low gas pressures (2 to 10 cm Hg). Large pulses due to heavy particle recoils, such as C recoils from the walls and C, O, and He recoils from the gas, are discarded. Small pulses due to secondary electrons produced by gamma rays are recorded and pulse height integrated. Maximum pulse-height discrimination between neutrons and gamma rays is obtained at or below pressures where the range of the C recoils is approximately the length of the sensitive volume of the counter.

Gamma-ray sensitivity (roentgens) is independent of energy to within 5 percent from 1.25 Mev (Co^{60}) to 200 kev and to within 20 percent down to 47 kev. Use of a graphite lining and a thin aluminum wall minimize production of gamma rays in the walls by inelastic scattering of the incident neutrons (which would lead to neutron sensitivity of the counter). Neutron sensitivity in a 2.5- to 3-Mev $H^2(d, n)He^3$ neutron field has been shown experimentally to be $\leq$ *1 percent of the first collision dose in tissue.* This type of instrument has relatively high sensitivity, and is therefore useful primarily at low gamma-ray dose rates below 10^{-2} rad/min.

d. Single Ionization Detector for Measurement of Gamma Radiation Only

The use of cavities to measure the energy absorbed in tissue from gamma radiation prescribes that the cavity be surrounded with materials having a low Z (Gray, 1936). Fast neutrons may transfer appreciable energy to these materials by elastic collisions. For example, it is seen (appendix 2) that the neutrons which transfer 1 rad to tissue will transfer to carbon 0.08 rad at 0.1 Mev and 0.25 at 10 Mev. If the amount of ionization produced in a small cavity inside a graphite medium were measured with the usual ionization current method, the ionization f_i due to neutron radiation capable of producing a dose of 1 rad in tissue, relative to the ionization due to gamma radiation capable of producing a dose of 1 rad in tissue, would be given by

$$f_i = F \times W_s/W_a, \tag{14}$$

where F is the ratio of the first collision dose in the medium which surrounds the cavity (in this case, graphite) to the first collision dose in tissue[7] for the same neutron field; W_e is the average energy dissipated per ion pair formed in the gas by electrons; and W_a is the average W value for the recoil atoms. Thus, if $W_e = W_a$, the neutron response of the ionization chamber would be between 10 and 20 percent in the range up to 10 Mev. Actually, W_a is very poorly known, hence f_t cannot be calculated with certainty.

The search for a method (Auxier, Hurst, and Zedler, 1958) of measuring ionization which could distinguish between that produced by the secondary electrons, generated by gamma rays, from that produced by recoil atoms led to the following considerations. Suppose that the linear dimension, t, of a cavity is very small and the gas pressure in the cavity is low so that the mean free path for ionization by electrons, λ_e, is much greater than t. This is equivalent to the statement that the probability of the electron making an ionizing collision in the gas is low. Hence, assuming that the number of ions produced obeys the Poisson distribution, to a good approximation each ionizing event leaves behind 1 ion pair. If each ionization can be detected, then the number of counts equals the number of ion pairs and the energy absorbed in the cavity is simply W_e times the number of counts.

On the other hand, for fast neutron recoils the mean free path for ionization, λ_a, may be much smaller than t under the same condition where $\lambda_e \gg t$, corresponding to the creation of a large average number of ion pairs, $\overline{N} = t/\lambda_a$ per traversal. The neutron response of the single ion detector as compared to gamma radiation is now given by

$$f_{sid} = \frac{f_t}{\overline{N}} = \frac{W_e}{W_a} \times \frac{F}{\overline{N}}. \tag{15}$$

But

$$\overline{N} = t/\lambda_a = \frac{t(dE/dx)_a}{W_a}; \tag{16}$$

hence,

$$f_{sid} = \frac{W_e}{W_a} \times \frac{W_a}{t(dE/dx)_a} \times F = \frac{W_e F}{t(dE/dx)_a}, \tag{17}$$

where $(dE/dx)_a$ is the stopping power for the recoil atoms. It is interesting to note that the poorly known quantity W_a is eliminated; however, the poorly known quantity $(dE/dx)_a$ is not eliminated.

[7] See appendix 2 for values of these quantities for various neutron energies.

The neutron response, f_{std}, is estimated for the case where the average cavity path, t, is set at 3 mm and the cavity is filled with 2.3 mm Hg of CO_2. The results are shown in table 4 where the values of $(dE/dx)_c$ are assumed to be the stopping powers found by Snyder and Neufeld for carbon ions (of energy E_c) in tissue (Snyder and Neufeld, 1957). The values of F in table 4 apply to fluorothene.

The design of a counter using these principles is shown in figure 19. The sensitive volume is a right cylinder with dimensions 0.5×0.5 cm (filled with CO_2 at 2.3 mm Hg) and lined with fluorothene.

At low X-ray and gamma-ray energies, the relative response per roentgen is greater than at higher energies, even with best operating conditions. This effect is presumably

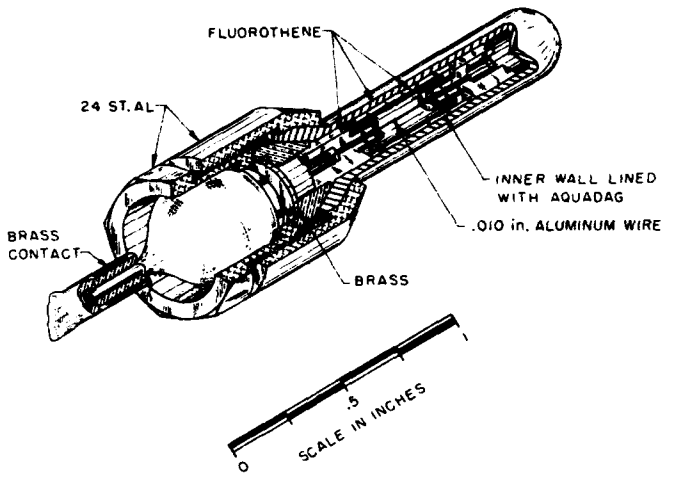

FIGURE 19. *Drawing for a gamma dosimeter using the single ion pair principle.*

due to the cross section for photoelectric interaction with high atomic number materials (such as the glass-metal seal near the sensitive volume). The response of a typical detector is given in figure 20 for several thicknesses of tin surrounding the cavity. With proper choice of the thickness of tin around the counter, its response is equal to that of ionization chambers down to about 100 kev. The counter

response for gamma radiation from Cs^{137} and Co^{60} remains the same as the response for the higher energy X-rays. A typical sensitivity value for counters of the above design is 1 mrad=500 counts; thus the use of the counters with the usual pulse amplifiers provides a useful range of sensitivity for radiation protection and radiobiological research.

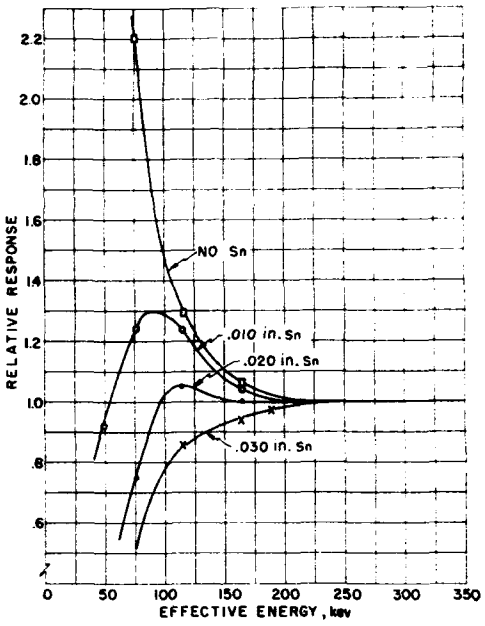

FIGURE 20. *X-ray response of the counter illustrated in figure 4.*

High response at low energies may be corrected with Sn.

TABLE 4. *Calculation of the neutron response of the single ionization detector*

E_n	F	$\bar{E}_r$	$(dE/dx)_n$	f_{std}
Mev	*Percent*	*Mev*	*kev/cm*	*Percent*
1.0	14.9	0.14	375	0.32
2.0	14.5	.28	600	.20
3.0	15.1	.42	1080	.15
4.0	24.7	.56	1600	.12
5.0	16.8	.70	2000	.07
10.0	34.1	1.4	3200	.085

e. Proportional Counter for Measurement of LET Distribution of Dose

A complete analysis of the radiation field for purposes of radiobiology and protection is one in which the dose delivered at each level of LET is determined. This information can be furnished in the form of a graph in which the dose per unit interval is plotted as a function of LET.

A method has been developed in which this "LET spectrum of dose" may be determined experimentally (Rossi and Rosenzweig, 1955a). The detector employed is a spherical proportional counter of tissue equivalent plastic. The particle spectrum set up in the wall of such a counter will be the same as the one occurring in tissue. The energy deposited by individual charged particles traversing the interior of the counter depends both on LET and the length of the track intercepted. However, the latter geometrical factor may be eliminated on a statistical basis with appropriate mathematical treatment of the pulse height curve that is obtained from the electronic equipment associated with the counter. The analysis is correct only if (1) particles traversing the cavity incur small change in LET and (2) particle trajectories are essentially straight lines. The first of these requirements may be attained by filling the counter with tissue equivalent gas at low pressure. The second requirement limits the use of the instrument primarily to positively charged nucleons and mesons. However, only for such particles can the RBE prescribed for protection purposes (NBS Handb. 59, 1954) be more than one. The mean LET of electrons is considered to be less than 3.5 kev/μ of water for purposes of personnel protection. The actual LET of electrons can attain values as high as 20 kev/μ. However, the range of electrons having a LET of more than 5 kev/μ is so short that traversal of the counter is impossible under the operating conditions usually chosen. Similarly, the total energy of such electrons is so low that pulses produced by them disappear in the noise. Because of the finite recovery time of the proportional counter, the radiation intensity that may be tolerated without undue "pile-up" is limited, particularly in the case of pulsed radiation sources. However, in the case of protection measurements the count rate recorded is usually adequately low.

Since the instrument is functional for essentially all charged particles having a RBE of more than one, and since the total tissue dose may be determined, using a tissue equivalent ionization chamber, a combination of these instruments may be used for complete analysis of the radiation field for purposes of protection.

Because of the principles of operation of this device, it is capable of a high degree of differentiation between particles of different LET. For particles of any given LET, only pulses corresponding to a major traversal need be counted, with those imparted by pulses due to shorter traversals being accurately predictable. This almost entirely eliminates the need for a low bias and makes it possible to evaluate the dose delivered by pulses that are normally lost in the electronic noise. Proper mathematical evaluation of the pulse height spectrum usually permits determination of the dose delivered between any two limits of LET. However, complications arise at neutron energies below about 200 kev because even if the instrument is operated at very low pressure, appreciable numbers of particles may stop or start in the cavity. However, at this point the whole concept of LET loses its meaning for biological structures having diameters less than 1 μ because of statistical fluctuations.

LET spectra obtained with this instrument (Rossi and Rosenzweig, 1955b) depend somewhat on the gas pressure within it and all differ from LET spectra based on theoretical computations. It has been shown (Rossi and Rosenzweig, 1956) that this effect is due to statistical variations of energy loss of charged secondaries and that such variations do, in fact, result in LET spectra which depend on the size of the "biological sample" to be evaluated. For purposes of protection such variations are usually of little consequence.

A limitation of the device is that with presently available models the maximum dose rate is of the order of 0.5 rad/hr. In addition, multichannel analyzers must be employed to obtain data from sources having variable intensity.

3.2. Chemical Methods

a. Photographic Film

(1) *Gamma rays.* The use of film for dosimetry of gamma rays is discussed by M. Ehrlich in NBS Handbook 57 (NBS, 1954). Photographic films and film badges such as the NBS film badge are widely used as gamma-ray dosimeters in mixed radiation fields. To evaluate the gamma-ray dose in a mixed field it is necessary to determine how much of the film blackening is due to neutrons. Ideally for this purpose one would like a film not to respond at all to neutrons so that blackening would be a measure of gamma radiation alone. Blackening due to thermal neutrons is produced by neutron activation of elements in the film such as silver which then decay by beta or gamma emission, the beta rays and the recoil electrons causing the blackening. For fast

neutrons the predominant cause of blackening is proton recoils from elastic scattering on hydrogen. Other processes, such as activation by fast neutrons and production of gamma rays by inelastic scattering on elements in the emulsion or packet, also contribute to blackening. Typical values for neutron sensitivity of NBS-type film badges are: Fast neutrons up to 3 Mev, 10 percent or less (on basis of first collision dose in tissue) of the gamma-ray sensitivity; and thermal neutrons, same order of sensitivity as for fast neutrons on the basis of incident flux of neutrons.

(2) *Thermal neutrons.* The predominant effect of thermal neutrons on photographic film is produced by the activation of the silver, two nuclides being formed, Ag^{108} and Ag^{110}, both of which decay by beta- and gamma-ray emission. The thermal neutron sensitivity of film may be enhanced by (1) incorporating lithium or boron into the emulsion leading to $Li^6(n,\alpha)$ or $B^{10}(n,\alpha)$ reactions, or (2) using external foils which, when activated by the thermal neutrons, irradiate the emulsion with beta rays or gamma rays. Use of rhodium foils leads to beta rays with an average energy of about 0.9 Mev. The only purely gamma-ray emitting foil extensively used in photographic dosimetry is cadmium. For further information on photographic film dosimetry, see Dudley (1956).

(3) *Fast neutrons.* Fast neutron dosimetry with photographic emulsions is almost exclusively done by track analysis with the advantages of higher sensitivity, less dependence on neutron energy, and good discrimination against gamma rays. The most reliable technique is a complete analysis of recoil proton number and energy, but this is very tedious. Cheka (1954), using the special counting method, has designed a device for which the number of tracks is proportional to dose over a wide range of neutron energies. This greatly simplifies the counting problem. Such arrangements have directional properties typically amounting to about a factor of two decrease in sensitivity when irradiated in the direction of the plane of the emulsion as compared to normal irradiation. A proton of 0.25 Mev energy has enough energy to generate a track of three grains—the minimum for recognition. The neutron energy range of Cheka's film packet has been extended from about 0.5 Mev (based on 0.25 Mev proton energy) to 14 Mev by covering the film with a sequence of cellulose and aluminum layers. A simpler device consisting of a 30 μ NTA emulsion surrounded by organic matter of 227 mg/cm^2 (film base, paper, etc.) is energy independent up to 3.5 Mev. For use in personnel monitoring one typically observes 12 to 25 micro-

scope fields. A dose of 0.1 rem (one-fiftieth of the average yearly maximum permissible neutron dose) is about 6 tracks in 25 microscope fields of area 2×10^{-4} cm^2. It is apparent from statistics that there is not much meaning to observations of doses smaller than this.

b. Liquid Chemical Systems

In considering chemical dosimetry of radiations it must be realized that the techniques available at the present time are at an early stage of development. In general nonchain chemical systems are restricted to total doses above 1,000 rads and in most cases to much higher values. Attempts to increase the sensitivity of these systems by the observations of very small changes in concentration have usually resulted in emphasized background effects, dependence on radiation intensity, and marked sensitivity to impurities. Similarly the introduction of systems involving chain mechanisms introduces these spurious effects as well as the possibility of an intensity dependence in the dosimeter. It may be expected that the future will see further development of chemical systems in the low dose region. For total doses above 1,000 rads a number of chemical systems are available which can be used to measure absorbed doses, particularly for gamma radiation, with a very high degree of accuracy.

(1) *The Fricke dosimeter—acid ferrous sulfate.* The chemical system which has been subjected to the most extensive study and on which most information is available at present is the oxidation of 0.001 molar ferrous sulfate in air-saturated 0.8N sulfuric acid solution (the Fricke dosimeter). The use of this dosimeter has been described in detail (Weiss, Allen, and Schwarz, 1956). Accurate measurements of absorbed dose in the 3,000 to 30,000-rad region can easily be carried out by direct spectrophotometric observation of the ferric ion produced. This system is usually used as the reference dosimeter for most radiation chemical reactions carried out with high energy X- and gamma radiation since its radiation yield has been absolutely calibrated for fast electrons and gamma rays both by calorimetric (Hochanadel and Ghormley, 1953; Lazo, Dewhurst, and Burton, 1954) and electrical energy input (Saldick and Allen, 1954; Schuler and Allen, 1956) methods. As a result of these calibrations, the value of G of ferrous oxidation may be taken as 15.5 $\pm$ 0.1 molecules/100 ev for electrons of an initial energy of approximately 2 Mev when completely stopped in the solution. For more densely ionizing radiations the yield drops considerably and approaches 3.6 for high LET. The detailed dependence of ferric ion production upon LET has been

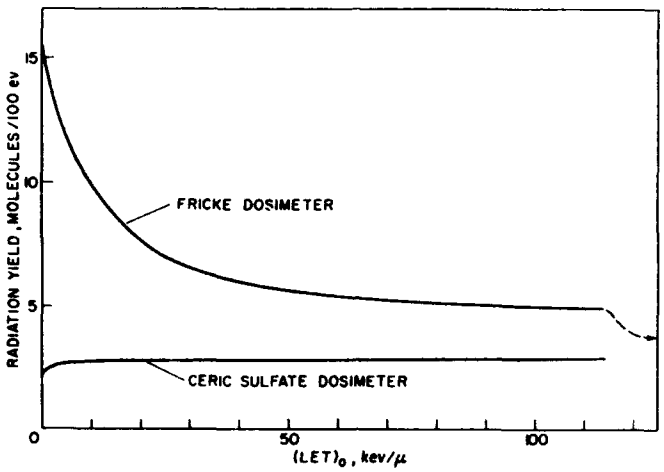

FIGURE 21. *Dependence of radiation yield of the Fricke (ferrous sulfate) and ceric sulfate dosimeters on initial LET.*

determined in an extensive series of experiments utilizing the charged particle radiations from a cyclotron (Schuler and Allen, 1957) and from nuclear reactions (Barr and Schuler, 1956) and is illustrated in figure 21. Because of this strong dependence of yield on LET in the region of interest for most fast neutron experiments this system is not generally useful in precise determinations of the total energy absorbed by the sample unless the energy spectrum of the neutrons is adequately known. However, because of the large difference between the radiation yields at high and low LET, this system is of some value for use in conjunction with other dosimeters for the determination of the relative importance of gamma and fast neutron contributions.

The ferric ion concentration may be conveniently determined by optical absorption measurements based on the Beer-Lambert relationship,

$$I/I_0 = 10^{-Elc}, \tag{18}$$

where I_0 and I are the initial and transmitted intensities at a particular wave length, l is the optical path length in centimeter, c is the concentration in moles/liter, and E is the molar extinction coefficient. The ferrous sulfate dosimeter is usually used in 0.8N sulfuric acid at which concentration the ferric ion extinction coefficient is found to be 2174 liter cm^{-1} $mole^{-1}$ at a wave length of 3050 A. With careful work,

Elc values of 0.001 can be detected with a 1-cm cell. This corresponds to c values of 5×10^{-7} mole/liter of ferric ion. Hence, by using the gamma radiation yield given above it is seen that this corresponds to an uncertainty in the dose determination of ±35 rads. If one employs 10-cm absorption cells and increases the effective extinction coefficient by the use of complexing agents such as thiocyanate, it is possible to make measurements which are accurate to ±10 percent at 25 rads. When care is used to employ distilled water free of organic impurities the ferrous sulfate system is quite stable and shows little oxidation over periods as long as one year.

(2) *Ceric sulfate.* The yield for reduction of cerium from valence four to three has been measured for fast electron and gamma irradiations and found to be 2.32 (Barr and Schuler, to be published). Measurements with beams of protons in the region of 10 Mev, of helium ions in the region of 40 Mev, and with boron (n, α) recoil radiation have given yield values of 2.7 to 2.9 for radiations having a LET ranging from 5 to 250 kev/μ, figure 21 (Barr and Schuler, to be published). This system therefore has considerable potential for measuring total energy dissipated in a sample if there is some knowledge of the relative contribution due to high and low LET radiations. The absorbed energy is given by the relation,

$$\text{Energy absorbed (in ev)}=\frac{\text{Molecules reacting}}{(0.023+0.005\,f)}, \quad (19)$$

where f is the fraction of the total energy absorbed which is due to fast neutrons. If no information on f is available, the choice of value of 2.6 for the radiation yield will give a measurement within 15 percent of the absolute value. Caution is urged, however, in the use of ceric sulfate as a dosimeter since this system is extremely sensitive to small amounts of impurities and can easily give erroneously high values of dose. Measurements in the absorbed dose range of from 5,000 to 50,000 rads are conveniently carried out by conventional spectrophotometric absorption techniques as described above. The molar extinction coefficient for ceric sulfate is 5,650 liter cm^{-1} $moles^{-1}$ at a wave length of 3,200 A.

(3) *The chloroform and tetrachloroethylene system.* The use of an acid liberating system in combination with a pH indicator appears to be attractive since if one starts with an unbuffered solution, concentration changes of the order of 10^{-6} mole are observable. Measurements can be carried out either colorimetrically or by titration of the liberated acid. Systems

based on these principles have been extensively investigated by Taplin and co-workers and formulations for actual dosimeters have been proposed (Taplin, 1956). These reactions involve formation of a long chain whose growth is severely inhibited by the presence of alcohol. The tetrachloroethylene system in particular has been suggested as one which should be sensitive to gamma radiation but relatively insensitive to fast neutrons (Sigoloff, 1956). In this system the radiation yield appears, from studies available to date, to be considerably lower for radiations of high LET. This lower response could result in the case of a chain reaction and suggests that dosimeters involving chain mechanisms might be further investigated for gamma-ray specificity. The tetrachloroethylene system, because of the lack of hydrogen, absorbs a relatively low amount of energy from the neutron beam. These combined factors account for the low-neutron response of tetrachloroethylene.

(4) *Quinine.* Recent studies by Barr and Stark (1958) have indicated that observations on the destruction of fluorescence of quinine in acid solution can be made at dose levels of 10 rads. These systems show considerable promise for estimates to even lower values. Solutions have been studied at concentrations down to 10^{-8} mole/liter where a dose of 150 rads results in a destruction of 50 percent of the fluorescence of the solution. Application to radiation of high LET is yet to be investigated but presumably will show a somewhat decreased response due to lower radical yields in the aqueous systems.

(5) *Hydrocarbon systems.* Preliminary investigations on a number of organic systems have given a strong indication that the radiation yields are considerably less dependent on LET than their aqueous counterparts. In particular the hydrogen yield from cyclohexane has been found to be the same within 5 percent for 12-Mev helium ion radiation (LET=50 kev/μ) and for 2-Mev electrons (LET=0.2 kev/μ) (Schuler and Allen, 1955). With the advent of gas chromatography it has become possible to measure small amounts of other components. Hydrocarbons and other organic systems should prove generally useful in the region above 10^6 rads.

(6) *Combinations of chemical systems in mixed radiation dosimetry.* The total energy deposited in a system can best be measured by a dosimeter whose response is independent of LET. Reactions based on the decomposition of aliphatic hydrocarbons are suggested as possibly showing the greatest promise for such a response characteristic. The use of the

ceric sulfate dosimeter, which shows a relatively small dependence on LET and is sensitive at somewhat lower total doses, appears to be a reasonably good approach. Combination of either of these systems with a dosimeter insensitive to high LET radiations gives a means of describing the fraction of energy deposited by each type of radiation, and combining a dosimeter having low response to high LET with the ceric sulfate dosimeter gives a means of evaluating f. With this value, it is possible to more accurately describe the total absorbed energy using the ceric sulfate system. At the present time no systems have been described which respond specifically to high LET radiations. In general, the chemical dosimetry of these radiations must be done by difference techniques; hence in many cases large errors are inevitable.

3.3. Dosimetry by Means of Spectral Measurements

a. Gamma-Ray Spectrometers

From a knowledge of the gamma-ray energy spectrum at a given point it is possible to calculate the dose that would be absorbed by a sample of material placed at that point. The first collision dose curves are given in appendix 1 for a number of low Z materials. In practice, the determination of the gamma-ray spectrum is so difficult that this method is virtually never used if only a dose determination is needed.

b. Neutron Spectrometers

Neutron dose may be evaluated by first determining the incident neutron spectrum, and then calculating the dose by use of the first collision dose curve or by using the results of a multiple collision dose calculation such as Snyder's in NBS Handbook 63 (NBS, 1957). However, it is usually much more difficult to measure neutron spectra than to measure the absorbed dose. Many spectrometers require knowledge of incident neutron direction; others cannot be used in a scattering medium (as in a phantom). A fortunate circumstance is that for measurement of absorbed neutron dose, high resolution is not necessary. This permits the use of threshold detectors and other relatively low energy resolution detectors. A more thorough discussion of the various types of neutron spectrometers than can be given here is contained in NBS Handbook 72 on Measurement of Neutron Flux and Spectra (1960).

(1) *Recoil counters.* Recoil counters usually make use of proton recoils from a thin hydrogenous radiator, the recoils being detected in a proportional or scintillation

counter or counter telescope. This method yields good resolution, but requires knowledge of incident neutron direction and is inefficient.

(2) Nuclear track emulsions. Nuclear track emulsions have been used perhaps more than any other method for the measurement of fast neutron spectra. Proton recoils are observed. The method has good energy resolution and efficiency but requires knowledge of incident neutron direction and involves tedious counting procedures. Attempts have been made to measure spectra by adding Li^6 to the emulsion and observing the alpha particles and the triton from the Li^6 $(n,\alpha)H^3$ reaction. This method may be used where incident neutron direction is not known (as in a moderator), provided there are not many low-energy neutrons present.

(3) *Threshold detectors.* Threshold detectors have been used (Hurst et al., 1956a) for approximate measurements of absorbed dose (by means of coarse spectral determinations) due to neutrons in the energy range between 5 kev and 10 Mev. They are suitable for high intensity bursts of neutrons where other detectors cannot be used. They do not require knowledge of incident neutron direction and may be used in a scattering medium.

In this method, Pu^{239}, Np^{237}, U^{238}, and S^{32} are used as the threshold detectors. Pu^{239} has a high fission cross section at thermal energies but this may be effectively removed by surrounding Pu^{239} with B^{10}. If Pu^{239} is surrounded with 2.2 g cm^{-2} of B^{10}, the effective cross section is about one-half maximum at 5 kev, and is essentially constant above 100 kev. One can determine in this way the total number of fast neutrons by measuring the number of fissions of Pu^{239}. The fission cross section for Np^{237} reaches one-half its plateau value at about 0.75 Mev, U^{238} at 1.5 Mev, and the S^{32} (n,p) reaction at approximately 2.5 Mev. These detectors provide enough data to make a reasonably accurate (± 10) calculation of tissue dose in many cases. The first collision dose is given by

$$D=[0.95(N_{Pu}-N_{Np})+2.4(N_{Np}-N_U)+3.0(N_U-N_S)+3.7N_S]\times 10^{-9} \quad (20)$$

where D is the tissue dose in rads; N_{Pu}, N_{Np}, N_U, and N_S are the numbers of neutrons per cm^2 with energy above the threshold for activation of Pu, Np, U, and S, respectively. This method leads not only to the total dose but also to the dose distribution with neutron energy.

The number of fissions which have been induced in the various fission detectors can be conveniently determined with scintillation counters. If two 2-in.×4-in. sodium iodide crystals are used (Reinhardt and Davis, 1958), the threshold detector method has the sensitivity shown in table 5. When neutrons capable of producing a dose of 10 rads in tissue are incident upon the detectors, the activities shown in table 5, column 2, will be produced. Column 3

TABLE 5. *Sensitivity of threshold detectors*

Threshold detector and effective threshold energy	Counts-min^{-1}-g^{-1} for 10 tissue rads of fission neutrons	Background (counts-min^{-1})	
		Counter	Sample (1 g)
Pu^{239} (Fast) [a]	[b] 2,325	300	1,000
Np^{237} (>0.75 Mev)	[b] 1,265	300	70
U^{238} (>1.5 Mev)	[b] 215	300	90
S^{32} (>2.5 Mev)	[c] 54	30	0

[a] Pu^{239} surrounded with 2 cm elemental B^{10} (density 1.1).
[b] At 1 hr after a short exposure to neutrons counted with two 2-in.×4-in. NaI counters, set to accept gamma rays above 1.2 Mev.
[c] S "burned" and counted according to Reinhardt-Davis technique (Reinhardt and Davis, 1958).

shows the background activity for the various detectors. In the case of S^{32} a very high sensitivity may be obtained by the sulphur burning technique developed by Reinhardt and Davis (1958). In this technique the sulphur samples are melted in an aluminum counting dish on a hotplate and ignited and allowed to burn completely. This process "burns off" essentially all the sulphur and leaves approximately 95 percent of the P^{32} in the aluminum counting dish.

In cases where neutron measurements are to be made near accelerators producing relativistic neutrons, two other threshold detectors are often used. Measurements with a 20-Mev threshold are made by detecting the $C^{12}(n,2n)C^{11}$ reaction in the carbon contained in 1,700-g cylinders of plastic scintillator (McCaslin, 1958) as suggested by the work with liquid scintillators of Baranov, Goldanskii, and Roganov (1957). The plastic scintillators in the forms of polished cylinders are first irradiated and then placed in contact with a 12.5-cm diam photomultiplier with an optical bond made by mineral oil. The counting is done inside a lead enclosure 10 cm thick. The cross section of the carbon reaction is roughly constant at a value of 22 mb from 50 Mev to more than 400 Mev (Baranov, Goldanskii, and Roganov, 1957).

An important feature of these detectors is that they are completely free of pile-up problems caused by the high instantaneous counting rates often encountered with electronic detectors such as ion chambers and proportional counters. A 1,700-g piece of plastic scintillator will give 100 disintegrations/min when the neutron flux over 20 Mev prior to counting has been 1 neutron/cm²/sec for a period of about three times the 20.4-min half life of the C^{11} formed. The cosmic-ray and natural background counting rate is about 1,000 counts/min (cpm). Greater sensitivity can be obtained by a proper selection of the minimum and maximum pulse heights that are counted and by using an anticoincidence cover of Geiger counters or scintillation counters over the scintillator while it is being counted, to reduce the background radiation.

Detectors with a 50-Mev threshold are used in the form of large fission pulse ion chambers (Hess, Patterson, and Wallace, 1957) containing effectively 60 g of Bi^{209} evaporated to a depth of 1 mg/cm² onto 42 aluminum plates 30 cm in diameter. The plates are connected by the components of a lumped constant delay line in such a way that a fission pulse originating between any pair of plates charges the capacity of only one pair of plates at a time, thus allowing 60,000 cm² of ion chamber area to be employed. The practical fission threshold for Bi^{209} is 50 Mev, and the cross section rises with energy to about 300 Mev and is then fairly constant up as far as it has been measured (Steiner and Jungerman, 1956; Sugarman, Campos and Wielgoz, 1956). The bismuth fission chamber is equally sensitive to neutrons and protons above 50 Mev and also to pions. One count is obtained when the chamber is exposed to 1 neutron/cm² (220 Mev).

Various methods have been used to determine the flux of neutrons in the thermal region. One of these methods uses the reaction $Au^{197}(n, \gamma)Au^{198}$ which is sensitive to neutrons in the thermal region but is also very sensitive to neutrons in the few ev (resonance) energy region. Cadmium-covered gold, however, is sensitive only to the resonance groups, hence the difference in the activation of bare gold and the activation of cadmium-covered gold is proportional to the thermal flux. Au^{198} decays by beta emission (0.97 Mev) followed by a 0.41-Mev gamma ray. Hence detection can be done either by beta or gamma counting. If a thin (0.005 in.), one-gram gold sample is gamma counted at optimum geometry with a 1½-in. by 1-in. NaI crystal counter set at an integral bias level of 0.35 Mev, the thermal neutron flux will be given approximately by

$$n/cm^2 = 1.7 \times 10^7 \times \text{counts/sec}, \quad (21)$$

assuming that the samples are counted at a time short compared to the half life of Au^{198}.

The thin foil technique provides a very simple means for determining the dose delivered to a medium of interest by charged particles. If one wishes to determine the first collision dose which results from the interaction of thermal neutrons with a biological sample, the foils may be placed at the particular point of interest and from their activation the thermal flux at that point may be calculated. For example, in tissue the energy absorbed from the $N^{14}(n,p)C^{14}$ reaction is easily determined by a first collision calculation. It is noted that the first collision calculation gives the correct value for the energy locally absorbed from the protons, but does not include the energy absorbed from the $H^1(n,\gamma)H^2$ reaction. The energy absorbed in the medium as a result of the gamma rays from this reaction may, however, be considered to be a part of the total gamma radiation field; hence, these gamma rays present no new difficulties.

(4) *Scintillation crystals.* Of the various fast neutron scintillation spectrometers, the $Li^6I(Eu)$ spectrometer of Murray (1958) would appear to hold exceptional promise for absorbed dose measurements since it has reasonable resolution, does not require knowledge of incident neutron direction, and may in principle be used in a phantom. This scintillator responds to the charged particles produced in the $Li^6(n,\alpha)T$ reaction. The resulting pulse height is proportional to the sum of the energy of the incident neutron and the energy released in the reaction (4.785 Mev). Because of this large positive Q value, an effective bias against gamma rays is provided. For optimum energy resolution, cooling of the Li^6I to liquid nitrogen temperatures is required.

3.4. Fast Neutron Dosimetry With Counting [8] Devices

The chief advantage of these methods is that the indication of energy absorbed in tissue may be obtained simply by counting the number of pulses (i.e., pulse height integration is not required) produced in a suitably designed detector.

a. Proportional Counters

In one of these examples (Hurst, Ritchie, and Wilson, 1951), a recoil proportional counter was designed to have a

[8] In the proportional counter methods referred to in section 3.1 the pulse heights are integrated to obtain the total amount of ionization formed in the gas-filled cavities, hence those methods do not fall in this category.

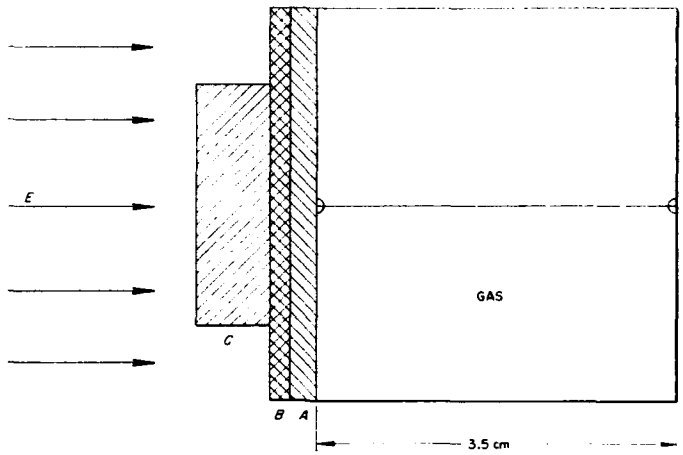

FIGURE 22. *Schematic of a fast neutron dosimeter using the special counting mehods.*

Three sources of recoil protons A, B, and C are combined in such proportions that the first collision dose curve is approximated.

count rate versus energy curve which approximates the first collision tissue dose curve. The energy response of the counter is determined by three sources of recoil protons (see fig. 22). Calculations were made of the probability that neutrons of energy E could cause a recoil proton to lose energy greater than the bias energy needed to discriminate against gamma radiation in the counting volume. The energy response curves for the three sources of protons are such that when added in the illustrated proportions of hydrogenous materials, the tissue first collision dose curve is approximated. The response has been checked experimentally with monoenergetic neutrons and agrees well with the theoretical curve. Gamma-ray interactions in the counter are easily discriminated against since the ionization in the counter due to secondary electrons is much less than the proton ionization. The chief disadvantage to this counter comes from the fact that the response is directional, being correct only when a plane beam is normally incident to the end of the counter.

Dennis and Loosemore (1957) have modified the above ideas to develop a proportional counter that is nondirectional in response. In this case the energy response curve follows the recommendations of the International Commission on Radiological Protection as given in British Journal of Radiology Supplement No. 6 (1955). At that time the permissible exposure was stated in terms of the absorbed energy at a depth of 2 cm below the surface of tissue.

b. Spherical Scintillator

Skjoldebrand (1955) has developed a spherical scintillation detector whose energy response is adjusted to the multiple collision absorbed dose curve of Snyder and Neufeld (1955b). Thus, this instrument indicates the maximum absorbed dose that a man would receive if located in the radiation field.

c. Plastics Loaded with Scintillating Crystals

The Hornyak button (Hornyak, 1952), which was developed for detection of fast neutrons, may be modified (Muckenthaler, 1956, 1957) to respond to fast neutrons in a manner similar to the dose absorbed in tissue (see appendix 2). Advantages which might lead to the use of this instrument arise from its relative insensitivity to gamma rays and from the simplicity of the instrument and the associated electronics.

In operation, fast neutrons striking the hydrogeneous material in the button produce proton recoils which in turn produce light from the ZnS which is detected in a photomultiplier. The range of a 1-Mev proton in ZnS is about 10 μ. The range of an electron of the same energy is about 10^3 μ. Hence by using particles of ZnS of a size comparable to the proton range and by employing dilute dispersions of these particles it is possible to discriminate against gamma-ray interactions since only a small fraction of the Compton electron energy will be dissipated in one particle of ZnS. The size and concentration of ZnS particles have been varied empirically on the basis of experiments with monoenergetic neutrons to produce an energy response to neutrons corresponding to the first collision dose curve for tissue.

This principle may be used to advantage with scintillators other than ZnS such as KI(Tl) and even grained plastic phosphors (Brown and Hooper, 1958). Advantages of these other scintillators include greater transparency, faster pulses, higher detection efficiencies, and atomic number closer to that of tissue. By the incorporation of boron in the inert plastic, or use of scintillating material such as LiI(Eu), it may be possible to construct a simulated dosimeter with

sensitivity to neutrons over the range from thermal energies to above 10 Mev. Gamma-ray discrimination is comparable to that of the Hornyak buttons.

d. Moderator Type Neutron Detectors

DePangher and Roesch (1955) and DePangher (1957) have shown that a paraffin moderator and BF_3 counter can be arranged in such a way that count rate is approximately proportional to first collision tissue dose rate over a range of neutron energies from 0.1 to 5.1 Mev. The arrangement is similar to the Hanson-McKibben (1947) long counter, but irradiation is done with neutrons incident normally to the axis of the cylinder. This type of device is very sensitive to neutrons and very effectively discriminates against gamma radiation; however, size and directional properties impose limitations on its application.

3.5. Intercomparison of Fast Neutron Dosimeters

Experiments have been performed to intercompare different types of fast neutron dosimeters. The dosimeters tested were: (a) The ethylene-polyethylene proportional counter, (b) the tissue-equivalent ionization chamber, and (c) the threshold detectors of Pu^{239}, Np^{237}, U^{238}, and S^{32}. The proportional counter and tissue-equivalent ionization chamber are both based on the Bragg-Gray cavity principle and in theory should have equal neutron responses. However, an important distinction arises in their method of measurement. In the proportional counter method an effective bias is provided against gamma radiation, and hence the proportional counter measures only neutron dose. On the other hand, the tissue-equivalent ionization chamber measures both the gamma and neutron components of tissue dose. Therefore, in order for comparisons to be made, the gamma dose component must be subtracted from the tissue-equivalent ionization chamber measurements. This requires an additional gamma measuring ionization chamber whose neutron response is accurately known. It is the uncertainty of the neutron response of the gamma measuring chamber which prevents any great precision for the intercomparison. In the early studies of Rossi et al., (1955) and Rhody (1956), this neutron response was neglected, and their results represented only a lower limit for the neutron tissue dose. Later, studies by Sayeg et al., (1958) have included an estimate of this response with the following assumptions: First, in a gamma-measuring chamber composed of a graphite wall and

CO_2 gas, the contribution of the carbon recoils from the graphite wall in producing ionization in the gas cavity is negligible; hence the total neutron response is due to the CO_2 gas. Second, the W values (ev/ion pair) for the heavy carbon and oxygen recoils in the CO_2 gas are the same as those for the low energy alpha particle. Table 6 shows the intercomparisons for four different sources. The proportional counter readings were normalized to unity and all dosimeters compared to the proportional counter. Within the experimental error of each method, the response was considered to be the same. The very close agreement found with the threshold detectors in the case of the fission spectrum (Sayeg et al., 1958; Reinhardt and Davis, 1958) would not be expected to hold in general because the number of different thresholds is too limited for adequate spectral resolution.

Choice of dosimeters compared in this section was based mainly on available data under comparable radiation conditions and not on relative merits of various methods.

TABLE 6. *Intercomparison of different fast neutron dosimeters*

Type of dosimeter	Rossi et al., (1955) monoenergetic neutrons from Van de Graaff (E_n=0.5 to 15 Mev.)	Rhody (1956) cyclotron neutrons from a Be target ($\bar{E}_n \cong 7$ Mev)	Sayeg et al., (1958) fission neutrons ($\bar{E}_n \cong 1.4$ Mev)	Reinhardt and Davis (1958) ORNL tower shielding facility—approximated fission spectrum
Proportional counter [a]	1.00	1.00	1.00	1.00
Tissue-equivalent Ionization chamber.	1.05 to 1.15	0.92 to 1.01	1.03 to 1.05	----------
Threshold detectors	----------	----------	0.97 to 1.02	1.01

[a] The proportional counter readings were arbitrarily taken as 1.00. The spreads in the other data reflect experimental errors or other uncertainties.

3.6. Remarks on Measurement of First Collision Dose and Absorbed Dose

It is pertinent to consider here the interpretation of instrument readings in terms of absorbed dose and first collision dose. These dose quantities and the relationship between them have been discussed in section 1.1. For purposes of measuring the absorbed dose in general, one needs a detector so small that it can be placed at any point of interest without disturbing the radiation field. The use of these devices, appropriately called "probe" dosimeters, is accompanied by a number of practical difficulties. As a consequence many devices are employed which measure the absorbed dose under particular or special circumstances.

For example, chambers designed under conditions of charged particle equilibrium are often too large to be satisfactory radiation probes. On the other hand, they may be used in air or "free space" to characterize the radiation field. In such cases the instrument reads a particular absorbed dose which depends on the constructional details of the detector. However, such readings may also be interpreted in terms of the first collision dose, particularly if the amount of material required to establish charged particle equilibrium is not so large that multiple interactions or absorption of incident radiation in it become important. Chambers constructed of ⅛ in. walls of tissue equivalent plastic (or polyethylene) may read about 5 percent less than the first collision dose for 0.5 Mev neutrons. On the other hand, the same chamber may read 15 percent higher than the first collision dose for 2 Mev neutrons (see appendix 2).

General comments relative to the applicability of some of the instruments discussed in this text to determination of absorbed dose and first collision dose are given below.

a. Tissue Equivalent Chambers

Most models contain very little material other than tissue equivalent plastic and they have been embedded in tissue equivalent solids or liquids when necessary. The gas volume required depends on the dose rate. In radiobiological work gas volumes are usually less than 2 cc and have been as small as 0.05 cc. In the case of first collision dose determinations, errors of the order of 10 percent must be expected below 2 Mev for chambers having $\frac{1}{16}$ in. walls. Chambers of this wall thickness have been used in radiobiological dosimetry. The ¼ in. wall chambers shown in the illustrations may be expected to require correction factors of the order of 20 to 30 percent at neutron energies up to perhaps 5 Mev.

b. Proportional Counters

The absolute dosimeter has a wall liner whose thickness is ⅛ in. For neutrons up to about 5 Mev, corrections of about 10 to 20 percent are required to convert the readings to first collision dose. Special designs (Hurst, 1954; Hurst et al., 1956b) are suitable for making absorbed dose measurements in tissue equivalent media.

c. LET Spectrometers

All chambers which have been built thus far have a minimum gas volume of at least 2 in. diam and they have not been used as yet in absorbed dose measurements inside phantoms.

The walls of all these devices have thus far been ¼ in. thick. Hence, they are subject to the same errors given above for tissue equivalent chambers having this wall thickness.

d. Threshold Detectors and Neutron Spectrometers

The type of corrections mentioned above do not apply to these methods since they depend on calculation of dose based on the measured spectrum. Either first collision dose or absorbed dose in general (including depth dose curves) can in principle be calculated from these measurements.

e. Special Counting Devices

The various special counting devices indicate first collision dose, maximum dose in a specified geometry, or doses applicable in protection, depending on design. In general, equilibrium arrangements are not employed; thus the type of corrections discussed above do not apply in these cases.

4. Summary and Applications

4.1. Radiobiology

Dosimetry for radiobiological research can be greatly facilitated by appropriate experimental design and it is therefore highly desirable that the individual responsible for dosimetry be consulted before the experiment is begun. Thus a common error which can easily be avoided results when biological material is exposed under conditions where radiation equilibrium is incomplete. Micro-organisms, plants and other thin biological objects should always be exposed under a sufficiently thick layer of material having the same or an equivalent atomic composition. Similarly, receptacles or supports should not contain significant amounts of markedly different elements (e.g., silicon in glass). Omission of these conditions results in a highly nonuniform distribution of absorbed dose which not only makes measurement much more difficult, but is usually also objectionable from the viewpoint of the biologist. Equally important modifications of the experimental arrangement may result when measures are taken to eliminate scattered radiation, to reduce the contribution of unwanted radiations (such as gamma radiation in a neutron experiment), to minimize spectral changes of the radiation originally emitted by the source (such as excessive moderation of a neutron source), and to insure a high degree of reproducibility of the physical exposure arrangement.

The level of dosimetric information required depends on the objectives of the biological experiment but past experience has shown that the information given is often insufficient. In many cases seemingly contradictory biological results have been shown to be due to differences in physical exposure conditions.

Certainly the minimum information required is the first collision dose. In the case of animals which are so large that attenuation is significant, the depth dose distribution in the animal is very desirable. Measurements of local variations of dose due to biological structures of different atomic composition (i.e., bone) are often important in radiobiological considerations but the required measurements are quite difficult and are hardly ever carried out.

When a biological object is exposed to a mixture of different types of radiation a separate assessment of the dose due to each is usually essential. Selective measurements of the dose in tissue due to neutrons may be carried out with the proportional counter, the LET spectrometer or paired ionization chambers.

Measurements of the LET distribution of dose can often be performed under conditions employed in radiobiology. However, because the technique is quite recent, this has been done only rarely. It is to be hoped that in future experiments LET distributions will be given, particularly in certain critical experiments such as evaluations of the RBE of fast neutrons.

There exist a number of parameters of the radiation field which influence dose and LET distributions. These include energy distribution of the radiation, half value layer and filtration. Whenever possible, information on such variables should be given. Table 7 lists instruments which may be useful in biological studies.

4.2. Radiation Protection

a. RBE Dose and the Rem

NBS Handbook 59 (1954) contains a discussion of the general principles and rules applicable to protection from external sources of ionizing radiation. NBS Handb. 60 (1955), NBS Handb. 54 (1954), NBS Handb. 55 (1954), and NBS Handb. 63 (1957) incorporate specific recommendations for conventional X-rays, gamma rays from radium, cobalt, and cesium, betatron and synchrotron radiations, and neutrons.

TABLE 7. *Summary of application of ionization chambers to mixed radiation dosimetry*

Descriptive name and reference	Radiation characteristics			Application				General comments
	Type	Energy range	Dose range [a]	*RB*	*RP*	*PS*	*ME*	
Tissue equivalent, Sec. 3.1.a	n γ	All neutrons X or γ	10^{-7} to 10^{3} s^{-1} in various sizes.	*E*	*E*	*N*	*D*	Can be made in various sizes to cover wide range of doses.
Carbon-CO_2 ref. 1, 2.								
900 cc	γ	X or γ	10^{-7} to 5×10^{-3} s^{-1}	*E*	*E*	*E*	*E*	Neutron response varies from about 10 percent at 1 Mev to about 30 percent at 14 Mev.
50 cc	γ	X or γ	5×10^{-6} to 10 s^{-1}					
4 cc	γ	X or γ	10 to 3×10^{3} s^{-1}					
Victoreen condensor types.	γ	X or γ	10^{-1} to 2.5×10^{3} in various sizes.	*E* (γ only)		*N*	*D*	Various dose ranges available. Special chambers for soft X-rays. Has large, but variable, neutron response.
Boron-lined pocket ion chambers.	n	Slow	0 to 0.06	*N*	*E*	*D*	*D*	Condenser type chamber designed for personnel monitoring. Sensitive to gamma radiation.
Absolute counter dosimeter, sec. 3.1.b.	n	Fast	Up to 10^{-2} s^{-1}	*E*	*E*	*E*	*N*	Calibrated with internal α source. Measures neutron dose in high gamma fields.
Secondary ethylene polyethylene types, sec. 3.1.b.	n	Fast	Up to 1 s^{-1}	*E*	*S*	*E*	*N*	Same as above except no internal α source.
Proportional counter dosimeter, sec. 3.1.c.	γ	X or γ	Up to 10^{-4} s^{-1}	*D*	*P*	*P*	*D*	High sensitivity to gamma rays. Low neutron response.
Single ionization detector, sec. 3.1.d.	γ	X or γ	Up to 5×10^{-3} s^{-1}	*P*	*P*	*D*	*P*	Very low response to neutrons. Measures gamma dose.
LET spectrometer, sec. 3.1.e.	n	Up to 100 Mev		*P*	*P*	*D*	*N*	Measures LET distribution for penetrating radiation.

Count rate dosimeter, sec. 3.4.a.	n	Fast	Biological tolerance ranges.	*D*	*E*	*D*	*D*	Indicates first collision, multiple collision, or maximum permissible dose, depending on design.
BF_3 counter + CH_2 moderator, sec. 4.2.d.	n	Fast	Up to 2×10^3 n/cm²/sec.	*N*	*S*	*S*	*D*	Measures fast neutron flux.
CH_2 lined proportional counter, sec. 4.2.d.	n	Fast	Up to 3×10^1 n/cm²/sec (at 1 Mev).	*N*	*S*	*S*	*D*	Measures fast neutron energy flux.
Spherical radiator with ZnS screen, sec. 3.4.b.	n	Fast	Up to 10^{-4} s^{-1}	*D*	*E*	*D*	*D*	Uniform directional response.
Hornyak button, sec. 3.4.c.	n	Fast	10^{-6} to 10^{-2} s^{-1}	*D*	*P*	*S*	*D*	Not completely investigated as dosimeter.
Anthracene crystals, ref. 3, 4, 5.	γ	X or γ	10^{-9} to 10^{-3} s^{-1}	*D*	*S*	*S*	*D*	Air equivalent above about 100 kev, depending on size of crystal. Large fast neutron response.
Threshold detectors (Pu, U, Np, and S), sec. 3.3.b.	n	Fast	> 1 when used as activation foils.	*E*	*E*	*S*	*E*	Give accurate dose values when spectrum *similar to* fission. Useful as area monitors where criticality can occur.
Threshold detector $C^{12}(n, 2n)C^{11}$, sec. 3.3.b.	n	> 20 Mev	Up to 10^4 n/cm²/sec	*S*	*S*	*S*	*N*	Very useful in radiation protection near high energy accelerators.
Threshold detector Bi^{209} (n,f), sec. 3.3.b.	n	> 50 Mev	Up to 10^6 n/cm²/sec	*S*	*S*	*S*	*D*	Very useful in radiation protection near high energy accelerators.
Au^{198} (n,γ) (with Au+Cd)	n	Thermal		*E*	*S*	*E*	*E*	One of the basic methods of *measuring thermal neutron* flux.
Photographic film, sec. 3.2.a.	γ	Depends on type	0.05 to 30,000	*S*	*E*	*D*	*D*	Accurate dosimetry requires very careful processing. Neutron response uncertain.

See footnote at end of table.

TABLE 7. *Summary of application of ionization chambers to mixed radiation dosimetry*—Continued

Descriptive name and reference	Radiation characteristics [a]			Application				General comments
	Type	Energy range	Dose range	*RB*	*RP*	*PS*	*ME*	
Nuclear track emulsion, sec. 3.2.a.	n	Fast	Biological tolerance ranges.	*S*	*E*	*D*	*D*	Cheka type packet gives dose by track counting.
Nonchain chemical systems, sec. 3.2.b.	γ	X or γ	$>1{,}000$	*E*	*D*	*D*	*E*	Fricke system often used as standard for radiation chemical studies.
Tetrachloroethylene chemical system, sec. 3.2.b.	γ	X or γ	>10	*E*	*S*	*E*	*E*	Low fast neutron response. Correction required due to energy dependence.
Phosphate glass, ref. 6	γ	X or γ	10 to 600	*S*	*S*	*D*	*P*	Probably has low fast neutron response. Correction required due to energy dependence.
Calorimetry	n	Any	$>10\ s^{-1}$	*P*	*D*	*D*	*E*	No discrimination of neutrons and gamma rays. Basic for radiation effects studies.
	X–γ			*E*	*D*	*D*	*E*	

[a] In the case of pulse counting techniques the upper limit for the dose rate or flux is such that the counting rate is 10^4 counts/sec.

References:

1. Ballweg and Meen, 1951.
2. Gray, 1944.
3. Carr and Hine.
4. McGown and Clifford.
5. Ramm, 1956.
6. Schulman, Shurcliff, Ginther, and Attix, 1953.

Key to Table 7

References

Sec.—denotes section in this report.
Ref.—denotes reference in this report.

Radiation Characteristics

n—denotes that an instrument is designed to measure neutrons.
γ—denotes that an instrument is designed to measure gamma rays.
Energy range—approximate indication of range of energy for which the instrument is primarily suited.
Dose range—refers to total dose in rads unless followed with s^{-1} which means rads per second.

Application

RB—radiation biology.
RP—radiation protection.
PS—neutron physics and shielding.
ME—materials (other than biological) effects.
E—extensively used in this field.
S—has been used as secondary method in this field.
N—not normally used in this field, although would be useful on special occasions.
D—utility in this field is doubtful.
P—use in this field is promising—applies particularly to new methods.

The permissible dose is specified in rems. The RBE dose in rems is equal to the product of the absorbed dose in rads and the RBE (relative biological effectiveness as used for purposes of protection) (NBS Handb. 63). Handbook 59 contains recommendations on RBE values as a function of the LET of charged particles. It is to be noted that these values are to be applied for chronic exposures of certain human critical organs for purposes of personnel protection. The RBE for X-rays, gamma rays, and electrons is taken to be 1. When tissue is exposed to neutrons the dose is delivered by particles having a wide range of LET and application of the recommendations in Handbook 59 requires rather complex computations. Snyder has performed such calculations for monoenergetic neutrons impinging normally on infinite slabs of tissue having a thickness of 30 cm. The results of this work form the

basis of the permissible neutron fluxes given in Handbook 63. Table 8 is a listing of these values.

TABLE 8. *Average yearly maximum permissible neutron flux*

Time-average flux for 2000 hr (assumed work year) to deliver 5 rems

Neutron energy	RBE and flux	Flux
Mev		$ncm^{-2}\ sec^{-1}$
Thermal	3	670
0.0001	2	500
.005	2.5	570
.02	5	280
.1	8	80
.5	10	30
1.0	10.5	18
2.5	8	20
5.0	7	18
7.5	7	17
10	6.5	17
10 to 30	----------	10 [a]

[a] Suggested limit.

b. Instrumentation

In some cases it is possible to employ in radiation protection essentially the same types of neutron dosimeters which are recommended above for radiobiological studies. In most instances, however, complete studies are not practical because of excessive time and effort required. Table 7 includes a list of instrumentation which has been designed primarily for protection measurements.

Radiation protection dosimeters are limited mainly to ionization type devices, which means that either the Bragg-Gray principle or the special counting concept is used in their design. If they are based on the Bragg-Gray principle the equilibrium condition is usually imposed so that the detector measures approximately the first collision dose. That is, the response of a small dosimeter of this type parallels the first collision curve and such a device should be calibrated in air, using first collision flux-dose conversions. Then, when an instrument is placed in air it will read the dose that a small mass of tissue would receive. The user should then realize that a man at this position would receive a range of doses for different parts of his body. Correction for this can be made by phantom measurements or by using depth dose data. Snyder and Neufeld (1955b) show that the buildup ratio,

$$\frac{\text{Maximum multiple collision dose for a man}}{\text{Maximum first collision dose}} \qquad (22)$$

is 1.6 ± 0.2 for fast neutron energies from 0.5 to 10 M

Many experimental investigations of depth dose distribution for X-rays have been carried out. Extensive data compiled by Glasser et al., (1952) and by the Scientific Subcommittee of the Hospital Physicists Association (Brit. J. Radiol., 1953), give air, surface, and depth doses for X-radiation of various qualities and beam widths in different materials. These data show relatively modest backscatter factors (1.0 to 1.5) for X-rays of up to 250 kev energy using various filters. This increase is caused by scattered X-rays. Data taken by Kock, et al., (1943) with 5, 10, 15, and 20-Mev gamma rays incident normally on a water phantom show a depth dose which peaks sharply below the surface of the phantom, giving a maximum dose which is 3.1 times the entrance dose for 20 Mev and 1.3 times the entrance dose for 5 Mev with intermediate values at the other energies. This increase is caused by the buildup of electronic equilibrium. The magnitude of the increase depends not only on the photon energy but also on the electron contamination of the incident photon beam.

Protection instruments may be designed which use the special counting concept such that they have a response parallel to the first collision dose curve or they may be designed such that they respond like the multiple collision curve. In the latter case the above considerations of dose buildup do not apply, since this information has effectively been "built into" the response of the instrument. In this case calibration is performed in the usual way with the exception that multiple collision flux dose conversions are employed.

c. Special Problem—Relativistic Neutrons

The neutrons produced by high-energy accelerators consist predominately of "evaporation" neutrons having energies of only a few million electron volts. While these neutrons must be considered in activation of materials inside the shield, they are eliminated by the first few inches of magnet structure or shielding and present no direct external hazard.

In addition to the evaporation neutrons, the accelerators produce high-energy neutrons in stripping, charge-exchange, and knock-on events in the target. These neutrons have energies ranging to the maximum energy of the accelerated particles. After these high-energy primaries have entered

the shielding, their spectrum is altered. There is first an initial building up followed by equilibrium with low-energy secondary neutrons that arise from evaporation events in the shielding. After equilibrium is established (i.e., after the peak of the buildup is passed), the neutrons of all energies are attenuated in direct proportion to the attenuation of the primaries, with no further change in the neutron spectrum. This shift of neutron energy toward lower values is so effective that the average energy of these neutrons present in biologically significant numbers outside such a shield may be in the neighborhood of 1 Mev. This energy shift makes it much easier to evaluate the neutron hazard than would be the case with the original high-energy neutrons.

The average energy of neutrons leaking through a biological shield may be estimated by either of two alternate methods. The first of these methods consists of taking two measurements, one of flux density and the other of energy flux density. Measurement of the neutron flux density is based on the counting rate with a BF_3 counter surrounded by 6.2 cm of paraffin (CH_2), both completely surrounded by a cadmium cover. The response of a BF_3 counter surrounded by this amount of paraffin has been measured and found to be essentially independent of energy over the range extending from a fraction of 1 Mev to about 20 Mev (Stephens and Smith, 1958). If a Hanson (Hanson and McKibben, 1947) "long counter" is available, it can also be used to approximate this energy-independent flux density if the nonisotropic sensitivity of this detector is taken into account.

An additional measurement is made with a polyethylene-lined proportional counter whose counting rate has been shown to be proportional to the neutron energy flux density between 0.1 and 20 Mev. The theory of the design and operation of this counter is described by Moyer (1952). After these two measurements have been made, the average neutron energy is obtained by dividing the energy flux rate by the flux rate.

The second of the two methods and frequently a simpler measurement of effective neutron energy requires the use of a BF_3 counter alone surrounded by various thicknesses of paraffin. The BF_3 proportional counter itself is sensitive primarily to thermal neutrons and, as paraffin is added around the counter, an increasing counting rate is observed until the paraffin becomes thick enough to absorb the thermal neutrons more effectively than it produces them from the incident flux of higher energies. After this thickness is exceeded, the counting rate will decrease as more paraffin is

added because of attenuation of the thermal neutrons. This buildup and subsequent reduction in counting rate depends upon the average energy of the neutrons as seen in figure 23.

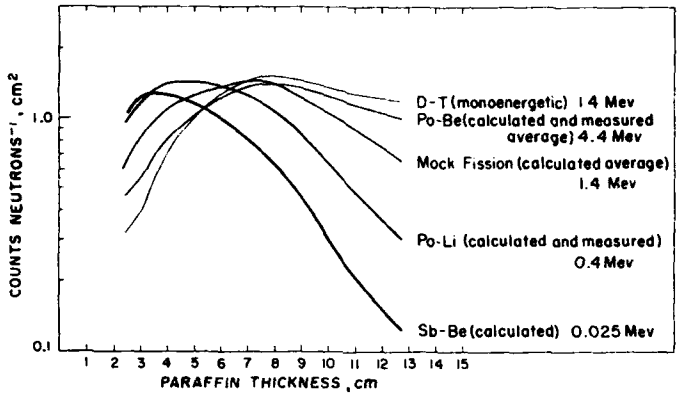

FIGURE 23. *Counting rate for a BF_3 proportional counter covered by various thicknesses of paraffin for five different neutron sources, corrected to an isotropic flux distribution (Hess and Smith, 1958).*

The counting statistics are more accurate than 1 percent.

Data plotted are the counting rates of a single BF_3 counter versus paraffin thickness. The paraffin in each case was covered with Cd and the data have been corrected to simulate an isotropic neutron flux. Five different neutron sources were used whose average energies varied from 25 kev to 14 Mev. The counting statistics are more accurate than 1 percent, but the process of averaging the data taken from different angles over the 4π solid angle possibly has introduced errors of as much as 10 percent. The DT neutrons are monoenergetic at 14.1 Mev. The Po-Be neutrons have a calculated and measured average energy of 4.4 Mev. The mock fission neutrons have a calculated average energy of 1.4 Mev. The Po-Li neutrons have a calculated and measured average energy of 400 kev. The Sb-Be neutrons have a calculated and average energy of 25 kev. By the use of these relations it is possible to obtain an effective neutron energy even in cases where the neutron flux is far below the presently accepted occupational permissible level because the sensitivity of a BF_3 counter is high.

In order to check the assumption that the major portion of the RBE dose outside of an accelerator shield is delivered by

neutrons in the energy range below 20 Mev in which the above two measurements are principally valid, two detectors whose threshold lie respectively at 20 and 50 Mev are often used (see sec. 3.3). It has been found that the large scintillators described in section 3.3 are especially convenient to use in performing a radiation survey. They are inexpensive to duplicate and may be simultaneously placed at many different locations. After exposure of the scintillators proper interpretation of the counting rate yields data from which isoflux radiation contours of the stray neutron field of a large accelerator may be plotted. The bismuth fission chamber is equally sensitive to neutrons and protons above 50 Mev and also to pions, but relatively few of these charged particles are present outside of a thick radiation shield. Thus, this detector is especially useful in measuring the flux of primary neutrons present outside the shielding.

A detector (Stephens, 1958) which has the advantage of inexpensive duplication (hence can be used in large numbers for mapping studies), is an In foil embedded in paraffin and surrounded by Cd. This assembly is a cubical box 15 cm on a side made of Cd 0.051 cm thick. Inside the box is a paraffin sphere 15 cm in diam made of two hemispheres. Each hemisphere has a central recess, 3.0 cm in diam and 0.3 cm deep in which an In foil is placed. The 0.125-mm thick foils used weigh about 500 mg each. The detector is sensitive to neutrons from 20 kev upward, with almost uniform efficiency from 0.4 to 20 Mev as seen in figure 23. The foils are counted in a methane-flow proportional counter, and when activated to saturation in the above assembly, a foil gives about 4 cpm for a fast neutron flux of 1 n/cm^2 sec. The counter has a background counting rate of 10 cpm. A flux as small as 3 n/cm^2 sec has been successfully measured with this detector. The response as a function of energy is similar to that of a BF_3 counter covered by 7.5 cm of moderating paraffin.

Measurements of the type described above may be made to establish the fact that in the case of interest most of the neutrons after penetration of the shield are no longer in the relativistic region but in the fast region. Absorbed dose may then be measured with methods applicable to the fast region. In many cases, however, the neutron flux and effective energy are used with the curves of Snyder in NBS Handbook 63 (1957) to estimate the biological hazard.

In the case of an experiment performed directly in a high energy neutron beam, of course no such degrading of the incident spectrum occurs, and the dose received by the ex-

perimental material is best calculated by the Monte Carlo method using the data outlined in section 1.1.c.

4.3. Shielding and Neutron Physics

a. Introduction to Shielding Measurements

Shielding measurements may be differentiated in several ways. One method would be with respect to the source of the radiation, i.e., accelerator, radioisotope, reactor, etc. Another breakdown may be made with respect to the type of object being protected by the shield. The protection of man has properly accounted for the vast majority of shielding studies. However, protection is also often required for instrumentation and materials. It should be, but has not always been, obvious that for such shielding requirements the dose absorbed in tissue or air may have no relevance whatsoever. Thus for experiments involving materials other than humans, the dose absorbed in the specific material should be determined. As will be discussed later, however, many of the effects produced by radiation are not directly related to the dose absorbed (see sec. 4.4).

Shielding measurements may also be divided into terminal and intermediate. Terminal measurements are those which are made after the radiation has penetrated the complete shield. Intermediate measurements would consist of those which are made after penetration of only a portion of the shield, i.e., within the shield. Such measurements are obviously most needed in complex shields which tend to be those of highest efficiency.

The object of the breakdown into terminal and intermediate measurements is to emphasize the following. For the terminal measurements the absorbed dose rate is the desired quantity. Thus, for terminal measurements the shielding applications of dosimetry become a part of the protection problem (see sec. 4.2). For the intermediate measurements, on the other hand, the desired quantity is not the absorbed dose rate but rather a spectral characterization of the radiation field. The desired parameters are the energy and angular distributions of the radiations at all points throughout the shield. Such measurements are difficult in general and have been impossible for most applications in the past. Only now are techniques becoming available (NBS Handbook 72, 1960), and many of these are not applicable for the mixed radiations emerging from a reactor shield. Consequently, in spite of the above considerations of the desirability of spectral data, much of the

present shielding technology has been based on measurements of absorbed dose rates using the instruments listed in table 7.

b. Problems in Shielding Dosimetry

The major problems encountered in shielding dosimetry instrumentation are those associated with measurements in mixed fields of neutrons and gamma rays. For the reasons discussed in section 4.3.a, separate determinations of the levels of each type of radiation are essential. Neutron measurements must often be made in the presence of a background of gamma radiation which exceeds the neutron level by a factor of 10^2 to 10^3. The requirements on the accuracy of dose-rate measurements for shielding are moderately severe. Errors less than 10 to 15 percent are usually desired.

c. Neutron Physics Applications

For monoenergetic neutron sources, flux determinations can be made using instruments which measure absorbed dose. However, great care must be exercised to minimize the energy degradation between the source and detector. The advantages which may justify such a measurement lie in the relative simplicity and availability of the necessary equipment.

4.4. Radiation Effects

a. Introduction

The modification of materials by radiation may be due to either ionization or displacement of atoms. Present information indicates that the ionization effects may be correlated with the absorbed dose but that displacement effects may not because they are proportional to the number of displacements produced and this number is strongly energy dependent. Thus the dose absorbed from two different spectra may have no relation to the number of displacements produced. For radiations with similar spectra but different magnitudes, the displacement effects should, of course, be proportional to the absorbed dose.

b. Ionization Phenomena

Ionization effects due to radiation tend to predominate when significant chemical changes can occur in the materials being irradiated. Thus, the polymers in plastics and elastomers have their character modified by cross linking and cleavage. Organic liquids such as lubricants undergo radiation-induced polymerization. Water is decomposed. Color-center phenomena darken glasses and alkali halides. All of the above materials are insulators. For metals,

ionization effects are negligible compared to displacement effects.

An additional effect of ionization is simply the bulk heating of the material. Such heating effects may assume great practical importance in exposures to reactor radiations.

All of the above ionization effects may be correlated with the doses absorbed in the material because the energy required to form an ion pair, for gasses at least, is virtually independent of the energy of the incident radiation. Secondary effects may arise from the rate of delivery of the absorbed dose. Thus the measurements desired to describe the radiation environment for insulators include a determination of the rate of dose absorption in the materials under investigation and a determination of the total dose absorbed. It may be desirable that the above measurements include a differentiation as to whether the dose was delivered by neutrons or gamma rays. In the usual reactor irradiation facility the absorbed doses contributed by neutrons and gamma rays are of the same order of magnitude.

c. Displacement Phenomena

Displacement phenomena include the production of vacancies, interstitials, impurities, and thermal spikes (Dienes and Vineyard, 1957). These interactions are produced by both neutrons and gamma radiation but neutron produced displacements predominate by a factor of the order of 100 or greater for equal absorbed doses. Gamma rays are relatively ineffective in displacement production because of the inefficiency of energy transfer from the zero rest mass photon to the relatively massive atom.

Displacement phenomena predominate in the radiation effects on semiconductors which occur at low-radiation levels, and in the effects on metals which occur at much higher radiation levels. Ceramics are damaged at levels intermediate between those mentioned above. Reactor fuels may be affected drastically by the displacements produced by the fission fragments. Similarly the neutron poisons such as boron will be subject to production of displacements due to the charged particles produced by neutron capture. The last two classes of reactions will yield an effect proportional to the thermal neutron flux incident on the material.

In the materials affected by atomic displacement phenomena a simple correlation of radiation effect with the absorbed dose would not be expected. Indeed, present theories do not agree concerning the influence on production

of displacements of the energy spectrum of the incident radiation (Seitz and Koehler, 1955; Kinchin and Pease, 1955; Snyder and Neufeld, 1955a, 1956). It appears that the number of displacements, and thus the radiation effect, may be approximately proportional to the energy absorbed for certain energy regions but the limits of these regions are uncertain. Further, all theories agree that such proportionality does not hold over all energy regions.

Since the displacement production by reactor radiations is predominantly due to neutrons, the data desired are primarily the energy distributions of the neutrons striking the material. The effect of the presence of the material upon the neutron spectrum must be considered.

d. Problems in Radiation Effects Measurements

The major problem encountered in measuring the effects due to neutrons is that the absorbed dose is not a suitable parameter for displacement production and thus the energy spectrum must be measured. Such spectral measurements are difficult and techniques are not fully developed (NBS Handbook 72 on Measurement of Neutron Flux and Spectra, 1960).

A problem which arises in the measurement of gamma-ray dose is damage to the dosimeter. In a flux level sufficiently high to produce measurable effects in materials, the detector may also be damaged. Thus plastic materials in an ionization chamber must be chosen for maximum radiation resistance and may still need to be periodically replaced. The necessary use of detectors of low sensitivity may give rise to spurious effects such as ionization within signal cables.

In the mixed fields of radiation encountered in reactors the problem of background rejection arises. The neutron-induced background must be evaluated and subtracted from a gamma-ray measurement and vice versa.

In many exposures the presence of the material undergoing irradiation may significantly perturb the radiation field. In this case, either measurements must be made with the material present or the perturbation must be calculated.

Table 7 includes some devices suitable for performing radiation effects dosimetry.

References

Amaldi, E., Bocciarelli, D., Cacciapuoti, B. N., and Trabacchi, G. C., (1946). Effetti di diffrazione nello sparpageliamento dei neutroni veloci. Nuovo Cimento **3**, 15. Also, Sullo sparpageliamento ellastico die neutroni veloci da parte di neuclei medi e pesanti, 203.

Auxier, J. A., Hurst, G. S., and Zedler, R. E., (1958). A single ion detector for measurement of γ-ray ionization in cavities. Health Physics **1**, 21.
Bakker, C. J., and Segre, E., (1951). Stopping power and energy loss for ion pair production for 340-Mev protons. Phys. Rev. **81**, 489.
Ballweg, L. H., and Meem, J. L., (1951). A standard gamma-ray ionization chamber for shielding measurements. ORNL–1028.
Baranov, P. S., Goldanskii, V. I., and Roganov, V. S., (1957). Dosimeter for high-energy neutrons. Rev. Sci. Instr. **28**, 1029.
Barr, N., and Schuler, R. H., (1956). Oxidation of ferrous sulfate by ionizing radiations from (n,α) reactions of boron and lithium. J. Am. Chem. Soc. **78**, 5756.
Barr, N., and Schuler, R. H., (to be published.)
Barr, N. F., and Stark, M. B., (1958). The destruction of the fluorescence of quinine in acid solution by 250-kvp X-rays. Radiation Research **9**, 89.
Bay, Z., Mann, W. B., Seliger, H. H., and Wyckoff, H. O., (1957. Absolute measurement of W_{air} for sulfur-35 beta rays. Radiation Research **7**, 558.
Bay, Z., and Newman, P. A., (to be published). Comparison of the ionization produced in air by alpha particles near 5 Mev and by beta particles. Radiation Research (in press).
Berger, R. T., (1960). The X-ray energy absorption coefficient tabulations and discussion (informal communication).
Bortner, T. E., and Hurst, G. S., (1953). Energy per ion pair for 5-Mev alpha particles in helium. Phys. Rev. **90**, 160.
Bortner, T. E., and Hurst, G. S., (1954). Ionization of pure gases and mixtures of gases by 5-Mev alpha particles. Phys. Rev. **93**, 1236.
Bratenahl, A., Fernbach, S., Hildebrand, R., Leith, C., and Moyer. B. J., (1950). Elastic scattering of 84-Mev neutrons. Phys. Rev, **77**, 597.
Bretscher, E., and French, A. P., (1944). British Atomic Energy Project Report 386; also, The measurement of a neutron flux in the presence of gamma rays. British Atomic Energy Project Report BR–517.
Bromley, D., and Herz, R. H., (1950). Quantum efficiency in photographic X-ray exposures. Proc. Phys. Soc. (London) **63B**, 90.
Brown, B., and Hooper, E. B., Jr., (1958). Plastic phosphor matrix for fast neutron detection. Nucleonics **16**, No. 4, 96.
Carr, R. T., and Hine, G. J., (1953). Gamma-ray dosimetry with organic scintillators. Nucleonics **11**, No. 11, 53.
Caswell, R. S., (1960). Neutron-insensitive proportional counter for gamma-ray dosimetry. Rev. Sci. Instr. **31**, 869.
Cheka, J. S., (1954). Recent developments in film monitoring of fast neutrons. Nucleonics **12**, No. 6, 40.
Cockroft, A. L., and Curran, S. C., (1951). The elimination of the end effects in counters. Rev. Sci. Instr. **22**, 37.
Dainty, J., (1950). Report on fast neutron dosimetry. CRM–482.
Davisson, C. M., and Evans, R. D., (1952). Gamma-ray absorption coefficients. Rev. Modern Phys. **24**, 79.
De Juren, J., (1950). Nuclear cross sections for 270-Mev neutrons. Phys. Rev. **80**, 27.
De Juren, J., and Knable, N., (1950). Nuclear cross sections for 95-Mev neutrons. Phys. Rev. **77**, 606.
Dennis, J. A., and Loosemore, W. R., (1957). A fast neutron counter for dosimetry. A.E.R.E. EL/R 2149.
De Pangher, J., (1957). Double moderator neutron detector. HW–54584.

De Pangher, J., and Roesch, W. C., (1955). A neutron dosimeter with uniform sensitivity from 0.1 to 3.0 Mev. Phys. Rev. **100,** 1793.
Dienes, G. J., and Vineyard, G. H., (1957). Radiation Effects in Solids. (Interscience Publishers, New York, N.Y.).
Dudley, R. A., (1956). Photographic film dosimetry, in Radiation Dosimetry. Hine and Brownell, editors. p. 300, (Academic Press, New York, N.Y.).
Failla, G., and Rossi, H. H., (1950). Dosimetry of ionizing particles. Am. J. Roentgenol. and Rad. Therapy **64,** 489.
Fano, U., (1954). Note on the Bragg-Gray cavity principle for measuring energy dissipation. Radiation Research **1,** 237.
Glass, F. M., and Hurst, G. S., (1952). A method of pulse integration using the binary scaling unit. Rev. Sci. Instr. **23,** 67.
Glasser, Quimby, Taylor, and Weatherwax, (1952). Physical Foundations of Radiobiology, 2d ed. (Paul B. Hoeber, Inc., New York, N.Y.).
Goldstein, H., (to be published). Nomenclature scheme for experimental monoenergetic nuclear cross sections. Appendix in Fast Neutron Physics, Eds., Marion and Fowler.
Gray, L. H., (1936). Ionization method for the absolute measurement of gamma-ray energy. Proc. Roy. Soc. (London) **156A,** 578.
Gray, L. H., (1944). The ionization method of measuring neutron energy. Proc. Cambridge Phil. Soc. **40,** 72.
Gray, L. H., and Mottram, J. C., and Read, J., (1940). Some experiments upon the biological effects of fast neutrons. Brit. J. Radiol. **13,** 371.
Greening, J. R., (1951). The photographic action of X-rays. Proc. Phys. Soc. (London) **64B,** 977.
Grodstein, Gladys White, (1957). X-ray attenuation coefficients from 10 kev to 100 Mev. NBS Circ. **583.**
Gross, W., Wingate, C., and Failla, G., (1956). Average energy expended in producing ion pairs—S-35, absolute value for air. Radiology **66,** 101.
Gross, W., Wingate, C., and Failla, G., (1957). Average energy lost by sulphur-35 per ion pair produced in air. Radiation Research **7,** 570.
Hadley, J., and York, H., (1950). Protons and deuterons ejected from nuclei by 90-Mev neutrons. Phys. Rev. **80,** 345.
Haeberli, W., Huber, P., and Baldinger, E., (1953). Arbeit pro ionenpaar von gasen and garmischungen fur X—teilchen. Helv. Phys. Acta. **26,** 145.
Hanson, A. O., and McKibben, J. L., (1947). A neutron detector having uniform sensitivity from 10 kev. to 3 Mev. Phys. Rev. **72,** 673.
Healey, R. H., and Reed, J. W., (1941). The Behaviour of Slow Electrons in Gases. (Amalgamated Wireless Valve Co., Sydney, Australia).
Hess, W. N., (1958). A summary of high energy nucleon-nucleon cross section data. Rev. Mod. Phys. **30,** 368.
Hess, W., Patterson, W., and Wallace, R., (1957). Delay-line chamber has large area, low capacitance. Nucleonics **15,** No. 3, 74.
Hess, W. N., and Smith, A. R., (1958). Private communication.
Hochanadel, C. J., and Ghormley, J. A., (1953). A calorimetric calibration of gamma-ray actinometers. J. Chem. Phys. **21,** 880.
Hoćrlin, H., (1949). The photographic action of X-rays in the 1.3 to 0.01 A range. J. Opt. Soc. Am. **39,** 891.
Hornyak, W. F., (1952). A fast neutron detector. Rev. Sci. Instr. **23,** 264.

Hughes, D. J., and Harvey, J. A. (1955). Neutron cross sections, BNL-325.
Hughes, D. J., Schwartz, R. B. (1958). Neutron cross sections. BNL-325, 2d edition.
Hurst, G. S., (1954). An absolute tissue dosimeter for fast neutrons. Brit. J. Radiol. **27,** 353.
Hurst, G. S., Harter, J. A., Hensley, P. N., Mills, W. A., Slater, M., and Reinhardt, P. W., (1956a). Techniques of measuring neutron spectra with threshold detectors-tissue dose determination. Rev. Sci. Instr. **27,** 153.
Hurst, G. S., Mills, W. A., Conte, F. P., and Upton, A. C., (1956b). Principles and techniques of mixed radiation dosimetry—application to acute lethality studies of mice with the cyclotron. Radiation Research **4,** 49.
Hurst, G. S., and Ritchie, R. H., (1953). A general purpose linear amplifier. Rev. Sci. Instr. **18,** 703.
Hurst, G. S., Ritchie, R. H., and Wilson, H. N., (1951). A count-rate method of measuring fast neutron tissue dose. Rev. Sci. Instr. **22,** 981.
International Commission on Radiological Protection, 1953 Report (1955). Brit. J. Radiol. Suppl. 6.
Jesse, W. P., and Sadauskis, J., (1955). Ionization in pure gases and the average energy to make an ion pair for alpha and beta particles. Phys. Rev. **97,** 1668.
Jesse, W. P., and Sadauskis, J., (1957). Absolute energy to produce an ion pair by beta particles from S-35. Phys. Rev. **107,** 766.
Jordan, W. H., and Bell, P. R., (1947). A general purpose linear amplifier. Rev. Sci. Instr. **18,** 703.
Kinchin, G. H., and Pease, R. S. (1955). The displacement of atoms in solids by radiation. Reports on Progress in Physics (Phys. Soc., London) **18,** 1.
Koch, H. W., Kerst, D. W., and Morrison, P., (1943). Experimental depth dose for 5-, 10-, 15-, and 20-million volt X-rays. Radiology **40,** 120.
Kruse, U. E., Teem, J. M., and Ramsey, N. F., (1956). Proton-proton scattering from 40 to 95 Mev. Phys. Rev. **101,** 1079.
Larson, H. V., (1958). Investigation of the energy loss per ion pair for protons in various gases. Phys. Rev. **112,** 1927.
Lazo, R. M., Dewhurst, H. A., and Burton, M., (1954). The ferrous sulfate radiation dosimeter: A calorimetric calibration with gamma rays. J. Chem. Phys. **22,** 1370.
Lea, D. E., (1947). Actions of Radiations on Living Cells. p. 7, (Macmillan and Co., New York, N.Y.).
Marinelli, L. D., (1953). Radiation dosimetry and protection, in Annual Review of Nuclear Science, Vol. 3, p. 249. (Annual Reviews, Inc., Stanford, Calif.).
McCaslin, J. B., (1958). High-energy neutron dosimeter. Health Physics **1,** 229.
McGown, F. K., and Clifford, C. E., (1951). Application of a scintillation detector to gamma-ray dosimetry. ORNL-CF-51-10-212.
Metropolis, N., Bivins, R., Storm, M., Turckevich, A., Miller, J. M., and Friedlander, G., (1958). Monte Carlo calculations on intranuclear cascades, 1. Low energy studies. Phys. Rev. **101,** 185.
Milvy, P., Genna, S., Barr, N., and Laughlin, J. S., (1958). Calorimetric determination of locally absorbed dose. Proc. International Conference on Peaceful Uses of Atomic Energy, (Paper 744).
Moe, H. J., Bortner, T. E., and Hurst, G. S., (1957). Ionization of acetylene mixtures and other mixtures by Pu^{239} α-particles. J. Phys. Chem. **61,** 422.

Moyer, B. J., (1952). Survey methods for fast and high-energy neutrons. Nucleonics **10**, No. 5, 14.
Moyer, B. J., (1954). Neutron physics of concern to the biologist. Radiation Research **1**, 10.
Muckenthaler, F. J., (1956). Applied nuclear physics annual progress report. p 199, ORNL–2081.
Muckenthaler, F. J., (1957). Applied nuclear physics annual progress report. p 270, ORNL–2389.
Murray, R. B., (1958). Use of $Li^6I(Eu)$ as a scintillation detector and spectrometer for fast neutrons. Nuclear Instruments **2**, 237.
National Bureau of Standards Handbook 54, (1954). Protection against radiations from radium, cobalt-60, and cesium-137.
National Bureau of Standards Handbook 55, (1954). Protection against betatron-synchrotron radiations up to 100 million electron volts.
National Bureau of Standards Handbook 57, (1954). Photographic dosimetry of X- and gamma rays.
National Bureau of Standards Handbook 59, (1954). Permissible dose from external sources of ionizing radiation.
National Bureau of Standards Handbook 60, (1955). X-ray protection.
National Bureau of Standards Handbook 62, (1957). Report of the International Commission on Radiological Units and Measurements (ICRU) 1956.
National Bureau of Standards Handbook 63, (1957). Protection against neutron radiation up to 30 million electron volts.
National Bureau of Standards Handbook 72 (1960). Measurement of neutron flux and spectra for physical and biological applications.
National Bureau of Standards Handbook on measurement of stopping power ratios, (to be published).
Nelms, A. T., (1953). Graphs of the Compton energy-angle relationship and the Klein-Nishina formula from 10 kev to 500 Mev. NBS Circ. **542.**
Ovadia, J., Danzker, M., Beattie, J. W., and Laughlin, J. S., (1955). Ionization of 9- to 17.5-Mev electrons in air. Radiation Research **3**, 340.
Ramm, W. J., (1956). Scintillation detectors, in Radiation Dosimetry. Hine and Brownell, editors, p. 259, (Academic Press, New York, N.Y.).
Randolph, M. L., (1957). Energy deposition in tissue and similar materials by 14.1-Mev neutrons. Radiation Research **7**, 47.
Reinhardt, P. W., and Davis, F. J., (1958). Improvements in the threshold detector method of fast neutron dosimetry. Health Physics **1**, 169.
Rhody, R. B., (1956). Fast neutron dosimetry at the Argonne National Laboratory cyclotron. Radiation Research **5**, 495.
Rich, M., and Madey, R., (1954). Range energy tables. UCRL–2301.
Richardson, R. E., Ball, W. P., Leith, C. E., and Moyer, B. J., (1952). Nuclear elastic scattering of high energy protons. Phy. Rev. **86**, 29.
Rossi, H. H., (1956). Neutrons and mixed radiations, in Radiation Dosimetry. Hine and Brownell, editors, p. 667, (Academic Press, New York, N.Y.).
Rossi, H. H., and Failla, G., (1950). Neutrons: dosimetry, in Medical Physics. O. Glasser, editor, p. 603, (Yearbook Publishers, Chicago, Ill.).

Rossi, H. H., and Failla, G., (1956). Tissue-equivalent ionization chambers. Nucleonics **14,** No. 2, 32.
Rossi, H. H., Hurst, G. S., Mills, W. A., and Hungerford, H. E., Jr. (1955). Intercomparison of fast neutron dosimeters. Nucleonics **13,** No. 4, 46.
Rossi, H. H., and Rosenzweig, W., (1955a). A device for the measurement of dose as a function of specific ionization. Radiology **64,** 404.
Rossi, H. H., and Rosenzweig, W., (1955b). Measurements of neutron dose as a function of linear energy transfer. Radiation Research **2,** 417.
Rossi, H. H., and Rosenzweig, W., (1956). Limitation of the concept of linear energy transfer (LET). Radiology **66,** 105.
Saldick, J., and Allen, A. O., (1954). The yield of oxidation of ferrous sulfate in acid solution by high-energy cathode rays. J. Chem. Phys. **22,** 438.
Sayeg, J. A., Larkins, J. H., and Harris, P. S., (1958). Experimental determination of fast and thermal neutron tissue dose. LA-2174.
Scharpe, J., (1952). Energy per ion pair for argon with small admixture of other gases. Proc. Phys. Soc. (London) **65A,** 859.
Schmieder, Karl. (1939). Bremsvermogen und Tragerbildung der X-Strahlen in Gasen. Ann. Phys. **35,** 445.
Schuler, R. H., and Allen, A. O., (1955). Radiation-chemical studies with cyclotron beams. J. Am. Chem. Soc. **77,** 507.
Schuler, R. H., and Allen, A. O., (1956). Yield of the ferrous sulfate radiation dosimeter: An improved cathode-ray determination. J. Chem. Phys. **24,** 56.
Schuler, R. H., and Allen, A. O., (1957). Radiation chemistry studies with cyclotron beams of variable energy: Yields in aerated ferrous sulfate solution. J. Am. Chem. Soc. **79,** 1565.
Schulman, J. H., Shurcliff, W., Ginther, R. J., and Attix, F. H., (1953). Radiophotoluminescence system of the U.S. Navy. Nucleonics **11,** No. 10, 52.
Seitz, F., and Koehler, J. S., (1955). The theory of lattice displacements produced during irradiation. Proc. International Conference on Peaceful Uses of Atomic Energy, (Paper 749).
Shonka, F. R., Rose, J. E., and Failla, G., (1958). Conducting plastic equivalent of tissue, air, and polystyrene. Proc. of Second International Conference on Peaceful Uses of Atomic Energy, (Paper 753).
Sigoloff, S. C., (1956). Fast neutron insensitive chemical gamma-ray dosimeter. Nucleonics **14,** No. 10, 54.
Skjöldebrand, R., (1955). A fast neutron scintillation counter with tissue response. J. Nuclear Energy **1,** 299.
Slater, M., Bunyard, G. B., and Randolph, M. L., (1958). Combination ion chamber-proportional counter dosimeter for measuring gamma-ray contamination of neutron fields. Rev. Sci. Instr. **29,** 601.
Snyder, W. S., and Neufeld, J., (1955a). Disordering of solids by neutron radiation. Phys. Rev. **97,** 1636.
Snyder, W. S., and Neufeld, J., (1955b). Calculation depth dose curves in tissue for broad beams of fast neutrons. Brit. J. Radiol. **28,** 342.
Snyder, W. S., and Neufeld, J., (1956). Vacancies and displacements in a solid resulting from heavy corpuscular radiation. Phys. Rev. **103,** 862.
Snyder, W. S., and Neufeld, J., (1957). On the passage of heavy particles through tissue. Radiation Research **6,** 67.

Spencer, L. V., and Attix, F. H., (1955). A theory of cavity ionization. Radiation Research **3,** 3.
Steiner, H. M., and Jungerman, J. A., (1956). Proton-induced fission cross sections for U-238, U-235, Th-232, Bi-209, and Au-197 at 100 to 340 Mev. Phys. Rev. **101,** 807.
Stephens, L., (1958). Fast neutron surveys using indium-foil activation. Health Physics **1,** 229.
Stephens, L. D., and Smith, A. R., (1958). Fast neutron surveys using indium foil activations. UCRL 8418.
Sugerman, N., Campos, M., and Wielgoz, K., (1956). Recoil studies of high-energy proton reactions in bismuth. Phys. Rev. **101,** 388.
Taplin, G. V., (1956). Chemical and colorimetric indicators, in Radiation Dosimetry. Hine and Brownell, editors, p. 357, (Academic Press, New York, N.Y.).
Tobias, C. A., Anger, H. O., and Lawrence, J. H., (1952). Radiological use of high energy deuterons and alpha particles. Am. J. Roentgenol. and Radium Therapy **67,** 1.
Valentine, J. M., and Curran, S. C., (1958). Average energy expenditure per ion pair in gases and gas mixtures. Reports on Progress in Phys. **21,** 1.
Wagner, E. B., and Hurst, G. S., (1958). Advances in the standard proportional counter method of fast neutron dosimetry. Rev. Sci. Instr. **29,** 153.
Wagner, E. B., and Hurst, G. S., (1959). Gamma response and energy losses in the absolute fast neutron dosimeter. Health Physics **2,** 57.
Weiss, J., and Bernstein, W., (1955). Energy required to produce one ion pair for several gases. Phys. Rev. **98,** 1828.
Weiss, J., Allen, A. O., and Schwarz, H. A., (1956). Use of the Fricke ferrous sulfate dosimeter for gamma-ray doses in the range 4 to 40 KV. Proc. International Conference on Peaceful Uses of Atomic Energy, (Paper 179).

Appendix 1. Calculations of First Collision Dose Versus Photon Energy

The first collision gamma-ray dose is defined in mathematical form by the equation,

$$D_f(E)=1.602\times10^{-8}[\sum_i\sigma_i N_i\epsilon_c+\sum_i\tau_i N_i\epsilon_{pe}+\sum_i k_i N_i\epsilon_{pp}] \quad (1)$$

where

$D_f(E)$=first collision dose for gamma rays in units of rads/photon/cm^2,

1.602×10^{-8}=conversion factor from Mev/g to rads,
σ_i=Compton scattering cross section per atom,
τ_i=photoelectric cross section per atom,
k_i=pair production cross section per atom,
N_i=number of atoms per gram of i^{th} species,
ϵ_c=average energy transferred to the electron undergoing Compton scattering.

$$\epsilon_c=\frac{\sigma_a}{\sigma_t}E_\gamma$$

where σ_a is the Compton energy absorption cross section, σ_t is the total Compton cross section, and E_γ is the energy of the photon.

ϵ_{pe}=average energy transferred to an electron formed by the photoelectric process $\epsilon_{pe}=E_\gamma-E_B$, where E_B is the binding energy of the electron, and

ϵ_{pp}=average energy transferred to the positive and negative electrons formed in the pair production process $\epsilon_{pp}=E_\gamma-1.022$.

Substituting

$$_a\sigma_m=\sigma_t N_t\times\frac{\sigma_a}{\sigma_t} \tag{2}$$

$$\tau_m=\tau_t N_t \tag{3}$$

$$K_m=k_t N_t\left(1-\frac{1.022}{E_\gamma}\right) \tag{4}$$

and

$$\mu_m={}_a\sigma_m+\tau_m+K_m. \tag{5}$$

Equation (1) reduces to

$$D_f(E)=1.602\times10^{-8}E_\gamma\textstyle\sum_i(\mu_m)_i. \tag{6}$$

The values of $D_f(E)$ are computed for different media (table A–1) in tables A–2, A–3, A–4, and A–5. Figures A–1, A–2, and A–3 show the continuous variation of $D_f(E)$ with photon energy. Values of $(\mu_m)_i$ were taken from table 1 of NBS Handbook 62 (1957).

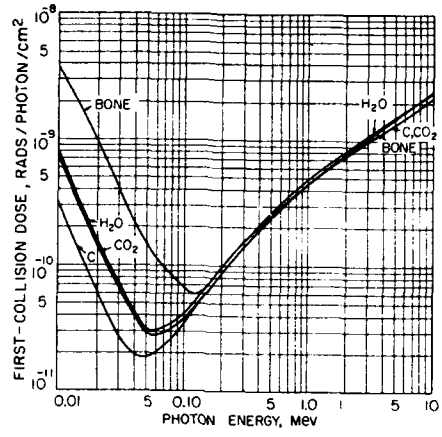

FIGURE A–1.

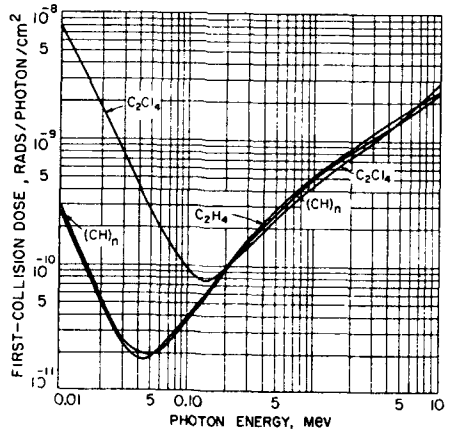

FIGURE A–2.

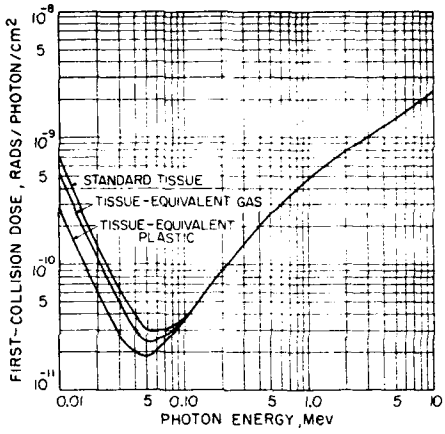

FIGURE A-3.

TABLE A-1. *Composition of media*

Material	Percent by weight								
	H	C	N	O	P	S	Cl	Ca	Other elements
Standard soft tissue [a]	10.0	12.0	4.0	73.0	[d] 0.2	[d] 0.2	------	[d] 0.01	[d] 0.59
Bone [b]	4.0	17.0	5.0	48.0	5.0	[d] 0.2	------	20.0	[d] 0.8
Tissue equivalent plastic	10.0	86.0	4.0	------	------	------	------	------	------
Tissue equivalent gas [c]	10.0	45.3	4.0	40.7	------	------	------	------	------
Water	11.2	------	------	88.8	------	------	------	------	------
Carbon	------	100.0	------	------	------	------	------	------	------
CO_2	------	27.2	------	72.8	------	------	------	------	------
$(CH)_n$	7.8	92.2	------	------	------	------	------	------	------
C_2H_4	14.4	85.6	------	------	------	------	------	------	------
C_2Cl_4	------	14.5	------	------	------	------	85.5	------	------

[a] Composition from Lea (1947).
[b] Wet bone, composition from Tobias (1952).
[c] This mixture contains 64.0 percent CH_4, 32.6 percent CO_2, and 3.6 percent N_2 by partial pressures.
[d] Elements neglected in calculations because of small abundance and small dose contribution.

TABLE A–2. *First collision dose relations for photons*

Photon energy	First collision dose (rad/photon/cm²×10⁻⁹)											
	Standard tissue					Bone						
	D_H	D_C	D_N	D_O	D_{Total}	D_H	D_C	D_N	D_O	D_{Ca}	D_P	D_{Total}
Mev												
0.01	0.000+	0.037	0.022	0.643	0.702	0.000+	0.053	0.027	0.423	2.880	0.321	3.70
.02	.000+	.008	.005	.137	.150	.000+	.011	.006	.090	0.802	.080	0.989
.03	.001	.003	.002	.057	.063	.000+	.005	.002	.037	.360	.030	.434
.05	.002	.002	.001	.024	.029	.001	.003	.001	.016	.122	.011	.154
.07	.004	.003	.001	.023	.031	.001	.004	.001	.015	.071	.007	.099
.10	.006	.004	.001	.027	.038	.003	.006	.002	.018	.036	.004	.069
.20	.017	.010	.003	.064	.094	.007	.015	.004	.042	.024	.005	.097
.30	.027	.017	.006	.101	.151	.011	.023	.007	.067	.031	.007	.146
.50	.047	.029	.010	.174	.260	.019	.040	.012	.114	.049	.012	.246
.70	.065	.039	.013	.240	.357	.026	.056	.016	.158	.066	.011	.333
1.0	.089	.053	.018	.328	.488	.036	.076	.022	.216	.089	.022	.461
2.0	.149	.090	.030	.547	.816	.059	.128	.038	.360	.150	.037	.772
3.0	.191	.118	.039	.723	1.07	.077	.167	.049	.475	.204	.049	1.02
5.0	.253	.163	.055	1.02	1.49	.101	.232	.069	.669	.320	.074	1.47
7.0	.302	.206	.070	1.31	1.89	.121	.292	.087	.861	.442	.099	1.90
10.0	.356	.263	.091	1.72	2.43	.142	.373	.114	1.13	.644	.140	2.54

TABLE A–3. *First collision dose relations for photons*

Photon energy	First collision dose (rad/photon/cm²×10⁻⁹)								
	Tissue equivalent plastic				Tissue equivalent gas				
	D_H	D_C	D_N	D_{Total}	D_H	D_C	D_N	D_O	D_{Total}
Mev									
0.01	0.000+	0.267	0.022	0.289	0.000+	0.141	0.022	0.359	0.522
.02	.000+	.056	.005	.061	.000+	.029	.005	.076	.110
.03	.001	.024	.002	.027	.001	.013	.002	.032	.048
.05	.002	.015	.001	.018	.002	.008	.001	.013	.024
.07	.004	.020	.001	.025	.004	.010	.001	.013	.028
.10	.006	.029	.001	.036	.006	.015	.001	.015	.037
.20	.017	.074	.003	.094	.017	.039	.003	.035	.095
.30	.027	.119	.006	.152	.027	.063	.006	.057	.153
.50	.047	.205	.010	.262	.047	.108	.010	.097	.262
.70	.065	.281	.013	.359	.065	.148	.013	.134	.360
1.0	.089	.384	.018	.491	.089	.202	.018	.183	.492
2.0	.149	.645	.030	.824	.149	.340	.030	.305	.824
3.0	.191	.843	.039	1.07	.191	.444	.039	.403	1.08
5.0	.253	1.17	.055	1.48	.253	.617	.055	.568	1.49
7.0	.302	1.48	.070	1.85	.302	.777	.070	.730	1.88
10.0	.356	1.89	.091	2.34	.356	.994	.091	.958	2.40

TABLE A–4. *First collision dose relations for photons*

Photon energy	First collision dose (rad/photon/cm²×10⁻⁹)						
	C	CO_2			H_2O		
	D_{Total}	D_C	D_O	D_{Total}	D_H	D_O	D_{Total}
Mev							
0.01	0.311	0.085	0.641	0.726	0.000+	0.782	0.782
.02	.065	.018	.137	.155	.000+	.167	.167
.03	.028	.008	.057	.065	.001	.069	.070
.05	.018	.005	.024	.029	.002	.029	.031
.07	.023	.006	.023	.029	.004	.028	.032
.10	.034	.009	.027	.036	.007	.033	.040
.20	.086	.023	.063	.086	.019	.077	.096
.30	.138	.038	.101	.139	.031	.123	.154
.50	.238	.065	.173	.238	.053	.211	.264
.70	.327	.089	.240	.329	.073	.292	.365
1.0	.447	.122	.327	.449	.099	.399	.498
2.0	.750	.204	.546	.750	.166	.666	.832
3.0	.980	.267	.721	.988	.214	.879	1.09
5.0	1.36	.370	1.02	1.39	.283	1.24	1.52
7.0	1.72	.467	1.31	1.78	.338	1.59	1.93
10.0	2.20	.597	1.71	2.31	.398	2.09	2.49

TABLE A–5. *First collision dose relations for photons*

Photon energy	First collision dose (rad/photon/cm²×10⁻⁹)								
	$(CH)_n$			C_2H_4			C_2Cl_4		
	D_H	D_C	D_{Total}	D_H	D_C	D_{Total}	D_C	D_{Cl}	D_{Total}
Mev									
0.01	0.000+	0.287	0.287	0.000+	0.266	0.266	0.045	7.67	7.72
.02	.000+	.060	.060	.001	.056	.057	.009	2.00	2.01
.03	.001	.026	.027	.001	.024	.025	.004	0.892	0.896
.05	.002	.017	.019	.003	.015	.018	.003	.287	.290
.07	.003	.021	.024	.005	.020	.025	.003	.171	.174
.10	.005	.031	.036	.009	.029	.038	.005	.093	.098
.20	.013	.079	.092	.024	.074	.098	.012	.084	.096
.30	.021	.127	.148	.040	.118	.158	.020	.119	.139
.50	.037	.219	.256	.068	.204	.272	.035	.196	.231
.70	.051	.301	.352	.094	.280	.374	.047	.268	.315
1.0	.069	.412	.481	.128	.383	.511	.065	.364	.429
2.0	.116	.692	.808	.214	.642	.856	.109	.614	.723
3.0	.149	.904	1.05	.275	.839	1.11	.142	.830	.972
5.0	.197	1.26	1.46	.364	1.17	1.53	.197	1.29	1.49
7.0	.235	1.58	1.82	.434	1.47	1.90	.249	1.73	1.98
10.0	.277	2.02	2.30	.512	1.88	2.39	.318	2.49	2.81

Appendix 2. Calculations of First Collision Dose Versus Neutron Energy

The first collision dose values included in tables A–6, A–7, A–8, and A–9 were calculated from the formula

$$D_f(E) = 1.602 \times 10^{-8} E_n \sum_i N_i \epsilon_i \sigma_i,$$

where

$D_f(E)$ = first collision neutron dose in rads/neutron/cm^2,

1.602×10^{-8} = conversion factor from Mev/g to rads,

E_n = energy of the neutron in Mev,

N_i = number of atoms/g of i^{th} species contained in the medium,

ϵ_i = fractional neutron energy transfer to the interacting nucleus; isotropic scattering in the center of mass system is assumed, and ϵ_i is equal to $2M/(M+1)^2$ where M is the mass of the nucleus, and

σ_i = elastic scattering cross section in barns (i.e., 10^{-24} cm^2).

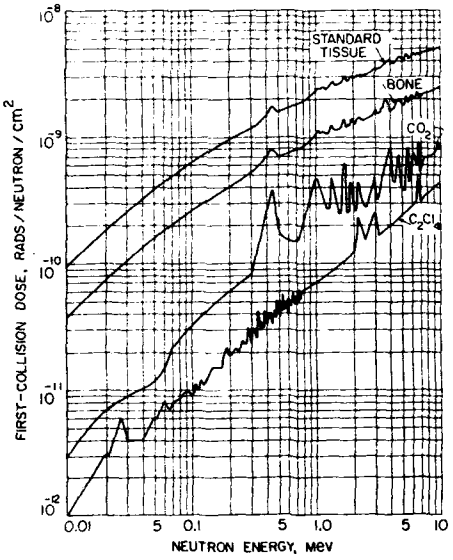

FIGURE A–4.

In these calculations the elastic scattering cross section was assumed to be isotropic and equal to the total cross section, since complete information is still lacking. All cross-section values were taken from D. J. Hughes and J. A. Harvey (1955). In table A–10 are included the values for the first collision dose values for 14.1-Mev neutrons based on the available nonelastic and elastic cross sections. The included graphs (figs. A–4, A–5, A–6, and A–7) show a more detailed analysis of the resonance dose values. Above 10 Mev the values become less accurate due to inelastic scattering, nuclear reactions, and anisotropy of elastic scattering.

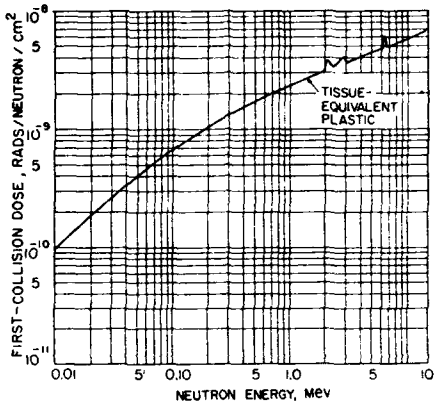

FIGURE A–5.

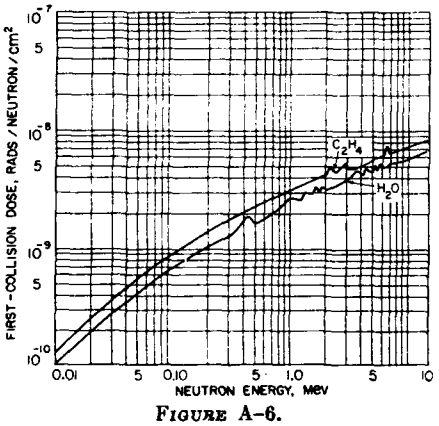

FIGURE A–6.

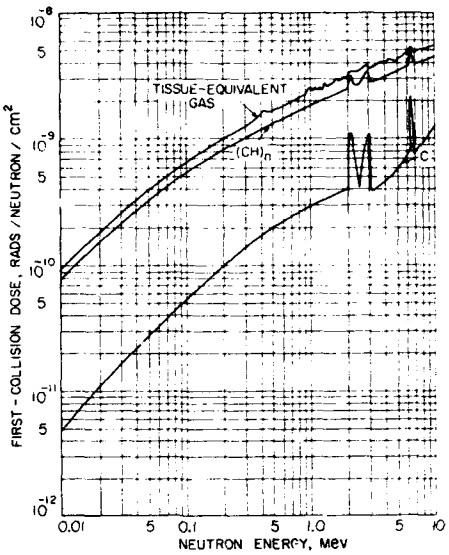

FIGURE A–7.

TABLE A–6. *First collision dose relations for fast neutrons*

Neutron energy	First collision dose (rad/neutron/cm²×10⁻⁸)											
	Standard tissue					Bone						
	D_H	D_C	D_N	D_O	D_{Total}	D_H	D_C	D_N	D_O	D_P	D_{Ca}	D_{Total}
Mev												
0.01	0.091	0.001	0.000+	0.002	0.094	0.036	0.001	0.000+	0.001	0.000+	0.000+	0.038
.02	.172	.001	.001	.004	.178	.069	.002	.001	.002	.000+	.000+	.074
.03	.244	.002	.001	.005	.252	.098	.003	.001	.003	.000+	.000+	.105
.05	.369	.003	.001	.008	.381	.148	.004	.001	.005	.000+	.000+	.158
.07	.472	.004	.001	.012	.489	.189	.006	.002	.008	.000+	.000+	.205
.10	.603	.006	.002	.017	.628	.241	.009	.002	.011	.000+	.000+	.263
.20	.914	.012	.003	.034	.963	.366	.016	.003	.022	.001	.000+	.407
.30	1.14	.016	.003	.052	1.21	.456	.023	.004	.034	.001	.001	.518
.50	1.47	.023	.004	.122	1.62	.588	.033	.005	.080	.001	.001	.707
.70	1.73	.029	.005	.089	1.85	.692	.041	.007	.059	.002	.004	.805
1.0	2.06	.036	.007	.390	2.49	.824	.051	.009	.2..	.003	.005	1.15
2.0	2.78	.047	.012	.156	3.00	1.11	.066	.015	.103	.006	.010	1.31
3.0	3.26	.045	.018	.205	3.53	1.30	.064	.023	.135	.009	.014	1.55
5.0	3.88	.079	.024	.244	4.23	1.55	.112	.030	.160	.012	.024	1.89
7.0	4.22	.094	.032	.485	4.83	1.69	.133	.041	.319	.015	.034	2.23
10.0	4.48	.157	.046	.595	5.28	1.79	.223	.057	.391	.018	.049	2.53
14.0	4.62	.259	.077	1.10	6.06	1.85	.367	.096	.720	.026	.070	3.13

TABLE A–7. *First collision dose relations for fast neutrons*

Neutron energy	First collision dose (rad/neutron/cm²×10⁻⁹)								
	Tissue equivalent plastic				Tissue equivalent gas				
	D_H	D_C	D_N	D_{Total}	D_H	D_C	D_N	D_O	D_{Total}
Mev									
0.01	0.091	0.004	0.000+	0.095	0.091	0.002	0.000+	0.001	0.094
.02	.172	.009	.001	.182	.172	.005	.001	.002	.180
.03	.244	.014	.001	.259	.244	.007	.001	.003	.255
.05	.369	.022	.001	.392	.369	.012	.001	.005	.387
.07	.472	.031	.001	.504	.472	.016	.001	.007	.496
.10	.603	.044	.002	.649	.603	.023	.002	.009	.637
.20	.914	.083	.003	1.00	.914	.044	.003	.019	.980
.30	1.14	.116	.003	1.26	1.14	.061	.003	.029	1.23
.50	1.47	.167	.004	1.64	1.47	.088	.004	.068	1.63
.70	1.73	.208	.005	1.94	1.73	.110	.005	.050	1.90
1.0	2.06	.255	.007	2.32	2.06	.135	.007	.217	2.42
2.0	2.78	.334	.012	3.13	2.78	.176	.012	.087	3.06
3.0	3.26	.324	.018	3.60	3.26	.171	.018	.114	3.56
5.0	3.88	.564	.024	4.47	3.88	.297	.024	.136	4.34
7.0	4.22	.673	.032	4.93	4.22	.355	.032	.270	4.88
10.0	4.48	1.13	.046	5.66	4.48	.593	.046	.332	5.45
14.0	4.62	1.86	.077	6.56	4.62	.978	.077	.611	6.29

TABLE A–8. *First collision dose relations for fast neutrons*

Neutron energy	First collision dose (rad/neutron/cm²×10⁻⁹)						
	C	CO_2			H_2O		
	D_{Total}	D_C	D_O	D_{Total}	D_H	D_O	D_{Total}
Mev							
0.01	0.005	0.001	0.002	0.003	0.102	0.002	0.104
.02	.011	.003	.004	.007	.193	.004	.197
.03	.016	.004	.005	.009	.273	.006	.279
.05	.026	.007	.008	.015	.413	.010	.423
.07	.036	.010	.012	.022	.529	.014	.543
.10	.051	.014	.017	.031	.675	.020	.695
.20	.097	.026	.033	.059	1.02	.041	1.06
.30	.135	.037	.052	.089	1.28	.063	1.34
.50	.194	.053	.122	.175	1.65	.148	1.80
.70	.242	.066	.089	.155	1.94	.108	2.05
1.0	.297	.081	.389	.470	2.31	.474	2.78
2.0	.388	.106	.156	.262	3.11	.190	3.30
3.0	.377	.103	.205	.308	3.65	.250	3.90
5.0	.656	.178	.243	.421	4.35	.297	4.65
7.0	.783	.213	.483	.696	4.73	.590	5.32
10.0	1.31	.356	.593	.949	5.02	.724	5.74
14.0	2.16	.588	1.09	1.68	5.17	1.33	6.50

TABLE A–9. *First collision dose relations for fast neutrons*

Neutron energy	First collision dose (rad/neutron/cm²×10⁻⁹)								
	$(CH)_n$			C_2H_4			C_2Cl_4		
	D_H	D_C	D_{Total}	D_H	D_C	D_{Total}	D_C	D_{Cl}	D_{Total}
Mev									
0.01	0.071	0.005	0.076	0.131	0.004	0.135	0.001	0.000+	0.001
.02	.134	.010	.144	.248	.009	.257	.002	.001	.003
.03	.190	.015	.205	.351	.014	.365	.002	.002	.004
.05	.288	.024	.312	.531	.022	.553	.004	.002	.006
.07	.368	.033	.401	.680	.031	.711	.005	.003	.008
.10	.470	.047	.517	.868	.044	.912	.007	.002	.009
.20	.713	.089	.802	1.32	.083	1.40	.014	.005	.019
.30	.889	.124	1.01	1.64	.116	1.76	.020	.005	.025
.50	1.15	.179	1.33	2.12	.166	2.29	.028	.013	.041
.70	1.35	.223	1.57	2.49	.207	2.70	.035	.017	.052
1.0	1.61	.274	1.88	2.97	.254	3.22	.043	.029	.074
2.0	2.17	.358	2.53	4.00	.332	4.33	.056	.074	.130
3.0	2.54	.348	2.89	4.69	.323	5.01	.055	.115	.170
5.0	3.03	.605	3.64	5.59	.562	6.15	.095	.169	.264
7.0	3.29	.722	4.01	6.08	.670	6.75	.114	.220	.334
10.0	3.49	1.21	4.70	6.45	1.12	7.57	.190	.262	.452
14.0	3.60	1.99	5.59	6.65	1.85	8.50	.313	.336	.649

TABLE A–10. *Energy deposition by 14.1-Mev neutrons*[a]

Media	First Collision dose (rad/neutron/cm²×10⁻⁹)					
	D_H	D_C	D_N	D_O	Other	D_{Total}
Standard tissue	4.64	0.29	0.09	1.64	0.01	6.67
Water	5.19	----------	----------	1.99	----------	7.18
$(CH)_n$	3.60	2.21	----------	----------	----------	5.81
C_2H_4	6.68	2.05	----------	----------	----------	8.73

[a] See Randolph (1957).

Submitted for the National Committee on Radiation Protection and Measurements.

Lauriston S. Taylor, *Chairman*

WASHINGTON, D.C., June 3, 1960.

U.S. GOVERNMENT PRINTING OFFICE: 1961